A diagrammatic approach for a clean multiferromagnetic Josephson junction

2007 J. Phys. A: Math. Theor. 40 12829

(http://iopscience.iop.org/1751-8121/40/43/002)

IOP PUBLISHING JOURNAL OF PHYSICS A: MATHEMATICAL AND THEORETICAL

J. Phys. A: Math. Theor. **40** (2007) 12829–12862 doi:10.1088/1751-8113/40/43/002

A diagrammatic approach for a clean multiferromagnetic Josephson junction

V Paltoglou, I Margaris and N Flytzanis

Department of Physics, University of Crete, PO Box 2208, 71003 Heraklion, Greece

Received 25 June 2007, in final form 11 September 2007
Published 9 October 2007
Online at stacks.iop.org/JPhysA/40/12829

Abstract

We consider a superconductor/multiferromagnet/superconductor (S/I/F_1/$\cdots$/F_n/I/S) ballistic junction with thin insulating layers in the interfaces. We develop a diagrammatic approach for the equation that determines the Andreev spectrum, by examining the closed loops in the intermediate ferromagnetic layers. It is expressed in terms of the S/F and F/F interface scattering amplitudes. A set of rules is determined. Several analytical formulas are obtained, and in particular we study the triple ferromagnetic layer case. We also obtain the maximum current from the scattering matrix, and show that it is consistent with the diagrammatic approach. A specific application is the asymmetric S/F/I/S junction. The diagrammatic approach is also checked with the matrix of scattering amplitudes method.

PACS numbers: 74.45+c, 74.78.Fk, 73.23.Ad

(Some figures in this article are in colour only in the electronic version)

1. Introduction

In a hybrid superconductor/normal/superconductor (S/N/S) Josephson system at low temperatures the flow happens by means of the Andreev reflection [1–3] mechanism, where an electron incident from the metal side and energy in the superconducting gap is reflected from the normal superconductor (NS) interface as a hole which has opposite charge, velocity and spin, while at the same time a pair is transmitted in the superconductor. At low temperatures they appear as *current-carrying bound states* of a multiply reflected electron–hole pair. The momentum mismatch at energy E of the electron–hole pair and the phase shift due to branch crossing processes determine these bound states [1, 3–6]. In the case of a ferromagnet in contact with an s-superconductor, the electrons and reflected holes in the ferromagnet, due to the opposite spins, get a Zeemann splitting from the exchange field E_{ex}. Thus even for an incident electron at the Fermi energy we have a momentum mismatch $\Delta p = \frac{2E_{\mathrm{ex}}}{v_f}$, which can be significant since in general $E_{\mathrm{ex}} \gg \Delta$. Thus, in an SFS junction, the relative phase increases

with the width of the ferromagnet d as $\Delta\Phi \sim \frac{2E_{\rm ex}d}{\hbar v_f}$ for the ballistic case. The exchange field leads to correlated pairs with nonzero total momentum and a significant decoherence in the electron and retroreflected hole at the FS interfaces [7–11]. This loss of coherence will affect phase sensitive quantities such as the spectrum of Andreev bound states and the supercurrent.

For clean interfaces and weak ferromagnets the basic mechanism of the bound states involves two Andreev reflections. At one interface from electron to hole and vice versa at the other interface forming a closed loop. Several analytic approximations can be obtained for the discrete Andreev spectrum, using the Andreev approximation [3, 10–13] for a single ferromagnetic layer if we neglect misfit between the bands in the layers, since we can neglect normal scattering. The discrete Andreev spectrum gives the dominant contribution to the supercurrent [4] for low temperatures. At higher temperatures the continuum spectrum must also be considered, and both can be included using the approach based on Green's functions [14].

On top of this we must also consider the quality of the interface, which can act as a normal potential, and the band misfit, which can lead to normal reflections. In general, we expect that the supercurrent depends on the various interface scattering amplitudes. One can develop a scattering matrix approach for the multilayer, in an iterative procedure, from which the supercurrent can be calculated. It is equally useful, however, to determine which are the important scattering processes and hope that the problem can be simplified in a systematic way by focusing on the dominant paths. The interface potential considered here can be extended to any potential which is homogeneous on the plane parallel to the interfaces, for which we know or can calculate independently the scattering matrix amplitudes. We do not consider the case of dirty junctions, which can be treated using quasiclassical Green's functions [10, 11].

Hybrid systems containing superconducting and ferromagnetic elements are actively studied experimentally with advances in junction preparation techniques. The effort is for well-characterized interfaces between ferromagnet and superconductors to study spin-dependent transport properties. Modern technologies for the preparation of layered structures by molecular beam epitaxy (MBE) allow the deposition of clean atomic thickness layers [15]. This provides the possibility of studying the coexistence and competition of ferromagnetism and superconductivity [10, 11]. In the S/F/S hybrid junction, an interesting experimental observation is the π-junction behavior which was predicted long time ago for the case of paramagnetic impurities [7] and observed experimentally [16–19]. The $0-\pi$ transition has also been studied theoretically in the clean [20–23] and diffusive [9, 24, 25] limit. The π junction is not a property only in SFS junctions. It can arise even with a non-magnetic material, by using nonequilibrium processes with a current injector in an appropriate geometry [26] with voltage control. It can also arise between two anisotropic high T_c superconductors [11], while along grain boundary junctions [27] one can have an interchange of 0 and π-junction regions. It is also created between anisotropic cuprate superconductor and an isotropic s-wave superconductor [28], while in a ramp junction of the same you can create π junctions at the step corners [29, 30]. Finally, the effect of an external magnetic field or from small nanomagnets [31] can also have a similar result. The case of a quantum dot between superconducting electrodes with resonant transport is also receiving attention [11]. Here we only refer to the case where the structure is layered.

Recently there has been strong interest in studying the effect of more than one layer and in particular the case of antiparallel polarization of the exchange field in the two layers. This is to see the effect on the dephasing and the conditions under which π-junction behavior is observed. The case of disorder has been extensively treated using the Usadel equations for the quasiclassical Green's function with several interesting results about the existence of π-junction for parallel or antiparallel exchange fields in the ferromagnetic layers. This is

done for S/F/I/F/S [20, 32–34] and S/F/F/S [35] Josephson junctions. In the latter case, the clean limit has also been considered for the collinear exchange field configuration. A piecewise constant spatial variation of the exchange field [36, 37] has also been considered, using a determinant expansion for the determination of the Andreev spectrum.

In this paper, we consider a multiferromagnetic layer with variable exchange fields and interface scattering as well as different band parameters. We develop a diagrammatic approach for both the determination of the Andreev bound states and the supercurrent, and obtain simple analytic expressions. This is achieved by the summation of the multiple scattering processes in a systematic way. This will indicate a selective summation of the important scattering processes, as determined by the strength of the various interface scattering amplitudes. For simplicity, we consider the problem in one dimension, but the diagrammatic approach is easily extended to take into account 3D junctions. In section 2 we present the model for the hybrid junction. In section 3 we sum all the closed scattering paths for the S/F/S junction and derive an expression for the condition for the Andreev spectrum. For the development of the method we also consider as an introduction the N/N/N/N junction. This gives all the necessary ingredients to consider the double ferromagnet junction, for which we can reproduce some analytic results in special limits. The summation of the closed paths is done using combinatorial techniques as sketched in the appendix. In section 4 we summarize the rules for dealing with a multilayer ferromagnet, and we apply them (in the appendix) to the case of a triple layer (S/F/F/F/S). Equivalently one can use the total scattering matrix [23], which is evaluated in the appendix. In section 5 we discuss the diagrammatic approach for the current and compare with the scattering matrix approach (for the total Andreev amplitude). This gives more physical insight than solving directly the Bogoliubov–de Gennes equations for a single [22] or a multilayered ferromagnetic [36] junction. In the last section we summarize our results.

2. The $S_L/I_L/F_1/I_C/F_2/I_R/S_R$ model

We consider a hybrid superconducting junction consisting of two bulk superconductors which are in contact with two thin insulating (oxide) layers and are separated by a nonsuperconducting region of total length d, which consists of n ferromagnetic layers $F_i, i = 1, \ldots, n$ of thicknesses d_i correspondingly. The superconductors can be different, as well as the ferromagnets. We assume a simple step-like spatial dependence of the order parameter, with $\Delta(z) = \Delta_\alpha(T)\,\mathrm{e}^{\mathrm{i}\phi_\alpha}$ with $\alpha = L, R$ for the left ($z < 0$) and right ($z > d$) superconductors and vanishing elsewhere ($\Delta = 0$ for $0 < z < d$). The phase difference of the order parameters is $\phi = \phi_R - \phi_L$. The temperature dependence of the bulk superconducting gap is $\Delta_\alpha(T) = \Delta_{0,\alpha} \tanh\left(1.74\sqrt{T_{c,\alpha}/T - 1}\right)$. The ferromagnetic layers are described within the Stoner model with the effective exchange energies $E_{\mathrm{ex},i}, i = 1, \ldots, n$ with parallel or antiparallel polarization to the junction interface. In the superconducting banks $V_\sigma(z) = 0$, i.e. we neglect the effect of the ferromagnet, which can be the case if the insulating layer is relatively strong. The exchange fields shift the Fermi levels of the two spin subbands and also cause ordinary reflections at the SF interfaces due to the Fermi energy mismatch. Except the exchange field misfit, the case of band parameter misfit is included.

In the absence of spin flip processes the two spin channels are decoupled for each set of solutions $(u_\sigma(z), v_{-\sigma}(z))$, and the BdG equations are

$$\begin{pmatrix} H_0 + V_\sigma(z) & \Delta(z) \\ \Delta^*(z) & -[H_0 + V_{-\sigma}(z)] \end{pmatrix} \begin{pmatrix} u_\sigma(z) \\ v_{-\sigma}(z) \end{pmatrix} = E \begin{pmatrix} u_\sigma(z) \\ v_{-\sigma}(z) \end{pmatrix}. \tag{1}$$

The diagonal terms of the BdG equations are written in the effective mass approximation

$$H_0 = -\hbar^2 \nabla \frac{1}{2m(z)} \nabla + V(z), \tag{2}$$

with uniform effective electron mass equal to m_S in the superconducting and ferromagnetic layers. All wavevectors will be normalized to the Fermi wavevector $k_{\mathrm{F}} = \left(\frac{2m_S E_{\mathrm{F}}}{\hbar^2}\right)^{1/2}$, with E_{F} being the uniform Fermi energy. Length is normalized to the coherence length ξ_0. Thus in the exponentials the dimensionless parameter $\kappa = k_{\mathrm{F}}\xi_0 = \frac{2}{\pi}\frac{E_{\mathrm{F}}}{\Delta_0}$ must be introduced.

The total potential consists of three terms $V(z) = W(z) + U(z) - \mu$, where $U(z)$ and μ are the electrostatic and the chemical potential, respectively, which have different but constant values in the layers of the junction. Scattering processes which are caused by the S/F and F/F′ interface insulating layers are modeled by delta-barrier potentials of the form $W(z) = Z_\alpha \delta(z - z_\alpha)$ for the two S/F interfaces at $z_L = 0, z_R = d$. The normal layer interfaces $\mathrm{F}_i/\mathrm{F}_{i+1}$ have corresponding strengths $Z_{i,i+1}$. In all cases the interface strength is normalized to $Z_F = E_{\mathrm{F}}/k_{\mathrm{F}}$, where the Fermi wavevector and energy are chosen in the left superconductor. Since we examine the behavior of the junction in the ballistic limit, no other scattering processes take place in the bulk of the layers due to disorder or spin-flip processes.

The BdG equations are easily solved in each layer and then matched at the interfaces. For the superconducting regions ($\alpha = L, R$) the solutions are

$$\psi_\alpha^{\pm e}(z) = \exp[\pm \mathrm{i}\kappa k_{\alpha,e} z] \begin{pmatrix} u_\alpha \, \mathrm{e}^{+\mathrm{i}\phi_\alpha/2} \\ v_\alpha \, \mathrm{e}^{-\mathrm{i}\phi_\alpha/2} \end{pmatrix}, \tag{3}$$

$$\psi_\alpha^{\pm h}(z) = \exp[\mp \mathrm{i}\kappa k_{\alpha,h} z] \begin{pmatrix} v_\alpha \, \mathrm{e}^{+\mathrm{i}\phi_\alpha/2} \\ u_\alpha \, \mathrm{e}^{-\mathrm{i}\phi_\alpha/2} \end{pmatrix}. \tag{4}$$

Here $\pm e(h)$ indicates the electron (hole)-like quasiparticle moving to the right(+) or left(−), $u_\alpha = \sqrt{(1 + \Omega_\alpha/E)/2}$ and $v_\alpha = \sqrt{(1 - \Omega_\alpha/E)/2}$ are the BCS amplitudes, and $\Omega_\alpha = \sqrt{E^2 - \Delta_\alpha^2}$. The normalized wavevectors are

$$k_{\alpha,p} = \left[1 \pm \mathrm{sign}(E)\frac{\Omega_\alpha}{E_{\mathrm{F}}}\right]^{1/2}. \tag{5}$$

In the ferromagnetic regions ($i = 1, \ldots, n$),

$$\psi_i^{\pm e}(z) = \exp[\pm \mathrm{i}\kappa q_{ei,\sigma} z] \begin{pmatrix} 1 \\ 0 \end{pmatrix}, \qquad \psi_i^{\pm h}(z) = \exp[\mp \mathrm{i}\kappa q_{hi,-\sigma} z] \begin{pmatrix} 0 \\ 1 \end{pmatrix}, \tag{6}$$

with the normalized wavevectors in each layer

$$q_{ei,\sigma} = \left[1 + \left(\frac{E}{E_{\mathrm{F}}} + \sigma\eta_i\right)\right]^{1/2} \tag{7}$$

$$q_{hi,-\sigma} = \left[1 - \left(\frac{E}{E_{\mathrm{F}}} + \sigma\eta_i\right)\right]^{1/2}. \tag{8}$$

We define the dimensionless exchange parameter $\eta_i = \frac{E_{\mathrm{ex},i}}{E_{\mathrm{F}}}$.

The scattering problem for the inhomogeneous structure has eight solutions when $E > \Delta$, which can be built up by combining the fundamental solutions in the different layers for a homogeneous material. From the interface matching conditions we obtain a matrix equation whose determinant, $\Gamma(E)$, will give us the Andreev bound states, when it vanishes. Here we

will develop a diagrammatic approach for finding the analytic expression, which will permit us to write Γ directly in terms of interface scattering amplitudes. The systematic procedure to be followed also allows us to introduce several possible limits in a direct way, as will be demonstrated in the following sections. The same determinant will arise in a scattering matrix approach, entering in the denominator as a result of summing multiple interface scatterings. The contribution of each diagram can be given in terms of the scattering amplitudes at F/F and S/F interfaces, which are given in the appendices in 7.1 and 7.2 correspondingly.

3. Denominator Γ as a summation of all multiple scatterings

The terms of the denominator Γ can be interpreted by diagrams. One could start and count all the possible closed loops in the scattering process. This is evident when one considers all the scattering paths with multiple scatterings in the determination of the scattering matrix. Our goal is to demonstrate that a diagrammatic approach can lead to closed and simple expressions for the denominator which include only a few basic terms with closed diagrams, which when expanded give all the possible paths. To develop the diagrammatic approach we will start from a simple four-layer normal superlattice $N_L/N_1/N_2/N_R$ where electrons and holes are disconnected. This will make it possible to show the summation procedure. The next step is to consider the simple S/F/S structure, where branch-crossing scattering processes make the closed loops more complicated, and this requires higher order closed loops to be included in the denominator. The procedure is extended to two intermediate ferromagnetic layers and then generalized to n-ferromagnetic layers. As special cases we consider the two- and three-layer structure in various limits to demonstrate that the diagrammatic approach is direct, once the algorithm is implemented. The final result will be given in terms of the scattering amplitudes for each interface separately.

3.1. The $N_L/N_1/N_2/N_R$ case

To demonstrate the diagram summation procedure, we start from a simple example of a junction consisting of four different non-superconducting regions labeled $(L, 1, 2, R)$, with different band and material properties, separated by three δ barriers of different strengths, Z_L, Z_{12} and Z_R. The widths of the intermediate layers are d_1 and d_2 correspondingly.

We can separate the closed paths traveled by the particles inside the interior of the junction according to the numbers of scattering events taking place at the outer barriers $(N_L/N_1, N_2/N_R)$. The summation over the closed paths includes all the multiple scatterings, and the goal is to express the total amplitude $\left(\sim\frac{1}{\Gamma}\right)$ in a closed form with $\Gamma = 1 - \gamma$. This means that we want to determine which closed paths contribute to γ. Thus, we will examine the sequence

$$\frac{1}{\Gamma^{(1)}} \to \frac{1}{\Gamma^{(2)}} \to \frac{1}{\Gamma^{(3)}} \to \frac{1}{\Gamma^{(4)}} \cdots \to \frac{1}{\Gamma^{(n)}}, \tag{9}$$

where $\frac{1}{\Gamma^{(n)}}$ includes closed loops with up to n reflections at the outer interfaces, i.e. for the sum of the powers in $[(r_{L1})']^{n_1}[r_{2R}]^{n_2}$, we have $n_1 + n_2 \leqslant n$. In the limit $n \to \infty$, we have

$$\frac{1}{\Gamma} \equiv \frac{1}{1-\gamma} = \lim_{n\to\infty} \frac{1}{\Gamma^{(n)}}. \tag{10}$$

First, we have two processes which have only one scattering event on the left or right outer barrier, which contribute to the amplitude by the factors

$$x_{N1} = ((r_{L1})' \, \mathrm{e}^{\mathrm{i}qd_1})(r_{12} \, \mathrm{e}^{\mathrm{i}qd_1}) = (\tilde{r}_{L1})'\tilde{r}_{12}$$
$$x_{N2} = ((r_{12})' \, \mathrm{e}^{\mathrm{i}qd_2})(r_{2R} \, \mathrm{e}^{\mathrm{i}qd_2}) = (\tilde{r}_{12})'\tilde{r}_{2R},$$

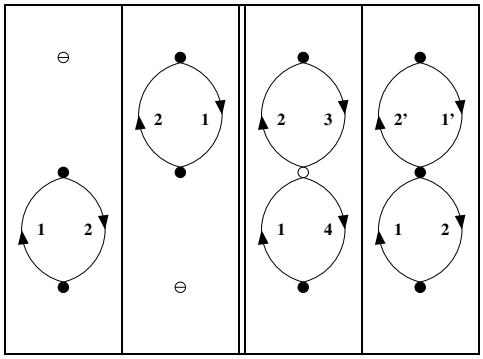

Figure 1. Processes x_{N1}, x_{N2}, x_{N3} and $x_{N1}x_{N2}$. The numbers next to the arrows indicate the order of propagation. The symbol (•) indicates an ordinary reflection, (○) indicates transmission (from both sides) and the (⊖) indicates that the interface is inactive. The layers are labeled $L, 1, 2, R$ from bottom up.

as seen in the first two columns of figure 1. In the above, we also include in the tilted scattering amplitudes the propagation factors. We use the convention (to be followed from now on) that the propagation factor is from the free propagation prior to the scattering event, i.e. in the unprimed amplitude the layer index (d_i) matches the first index in the amplitude, while in the primed it matches the second index. So the expansion to first order in the scattering events at the outer interfaces is

$$\frac{1}{\Gamma^{(1)}} = 1 + x_{N1} + x_{N2}.$$

The term x_{N1} (in layer N_1) has a scattering event at the left interface and no scattering event at the right interface. We will call the left interface active, symbolized with •, and the right inactive, symbolized with ⊖. For the loop x_{N2} (in layer N_2), the right interface is active and the left is inactive.

Next, consider the loops which consist of two reflections at the outer interfaces, involving $(\tilde{r}_{L1})'$ or $\tilde{r}_{2R}$. We have four possible loops with relative amplitudes

$$\begin{aligned} x_{N1}^2 &= ((\tilde{r}_{L1})'\tilde{r}_{12})((\tilde{r}_{L1})'\tilde{r}_{12}) \\ x_{N2}^2 &= ((\tilde{r}_{12})'\tilde{r}_{2R})((\tilde{r}_{12})'\tilde{r}_{2R}) \\ x_{N1}x_{N2} &= ((\tilde{r}_{L1})'\tilde{r}_{12})((\tilde{r}_{12})'\tilde{r}_{2R}) \\ x_{N3} &= (\tilde{r}_{L1})'(\tilde{t}_{12})'\tilde{r}_{2R}\tilde{t}_{12}. \end{aligned} \tag{11}$$

The last term x_{N3} (third column in figure 1), although it is strictly speaking a second-order process, cannot be decomposed into a product of first-order processes, and for this reason we will call it a basic process along with x_{N1} and x_{N2}. Now the expansion to second order is

$$\frac{1}{\Gamma^{(2)}} = 1 + x_{N1} + x_{N2} + x_{N3} + x_{N1}^2 + x_{N2}^2 + x_{N1}x_{N2}.$$

We can rewrite this as

$$\begin{aligned} \frac{1}{\Gamma^{(2)}} &= 1 + (x_{N1} + x_{N2} + x_{N3} - x_{N1}x_{N2}) + x_{N1}^2 + x_{N2}^2 + 2x_{N1}x_{N2} \\ &= 1 + \gamma + x_{N1}^2 + x_{N2}^2 + 2x_{N1}x_{N2}, \end{aligned}$$

where

$$\gamma = x_{N1} + x_{N2} - (x_{N1}x_{N2} - x_{N3}), \tag{12}$$

while the term $x_{N1}^2 + x_{N2}^2 + 2x_{N1}x_{N2}$ will be included as part of γ^2. Considering all multiple scattering events and similar rearrangements as above (see appendix in A.3), we are able to complete exactly all powers of γ, so that

$$\frac{1}{\Gamma} = 1 + \gamma + \gamma^2 + \cdots = \frac{1}{1-\gamma}. \tag{13}$$

Thus we see that the contribution in the denominator of Γ comes from the basic processes x_{N1}, x_{N2} (first-order scattering), x_{N3} (second-order scattering), and the secondary process $x_{N1}x_{N2}$, but with a negative sign. In the last two diagrams of figure 1, the intermediate interface is connected to both (outer) neighboring interfaces and is named doubly linked, while in the first two diagrams it is connected only to one of the outer interfaces and is called singly linked. Finally, the contribution of the two diagrams in Γ can be described by

$$x_{N1}x_{N2} - x_{N3} = (\tilde{r}_{L1})'\tilde{r}_{2R}(\tilde{r}_{12}(\tilde{r}_{12})' - \tilde{t}_{12}(\tilde{t}_{12})') = (\tilde{r}_{L1})'\tilde{r}_{2R}g_{N12},$$

where we associate

$$g_{N12} = \tilde{r}_{12}(\tilde{r}_{12})' - \tilde{t}_{12}(\tilde{t}_{12})', \tag{14}$$

with the double-linked N_1/N_2 interface.

With the same procedure one could reproduce the denominator if the carriers in the normal regions would be holes. To distinguish electrons from holes we use a superscript e, h and draw paths traveled by holes with dashed lines. Consider now that electrons and holes both are present in a metal and solve the problem with no coupling between them. The denominator of this system is

$$\frac{1}{\Gamma} = \frac{1}{(1-\gamma^e)(1-\gamma^h)}. \tag{15}$$

We discussed this simple case in detail only to demonstrate the practical steps which will be followed in the more complicated case, where the outer layers are superconducting and will couple electrons and holes in the intermediate layers.

3.2. The S/F/S case

If we assume now that the outer regions (L, R) are in the superconductingting state, new scattering possibilities arise. Andreev processes can take place, that is, electrons can be scattered into holes and vice versa. Let us examine first the S/F/S junction. Again we consider the closed diagrams. The processes consist now from two or four reflections at the SF interfaces, where they can be either normal ($e \to e, h \to h$) or Andreev ($e \to h, h \to e$). The loops with two scattering events are shown in figure 2, where now we consider in parallel electron (continuous lines) and hole (dashed lines) propagation. At each interface, we introduce two vertices that describe scattering events of incident electrons and holes correspondingly. The vertices on the same interface are connected with the Andreev process. To denote that a vertex is Andreev reflection active we use the symbol $\bigotimes$. In the first (second) diagram, we have normal electron (hole) reflections with inactive vertices at the hole (electron) side. Their corresponding contributions are x_1 and x_2. Note that the auxiliary quantities x_i for $i = 1, 2, \ldots$ have a different definition here than the corresponding x_{Ni} defined in the N/N/N/N case. The other two diagrams in figure 2 correspond to Andreev reflections at the two interfaces and give the contributions x_3 and x_4. This is demonstrated by the horizontal lines that connect the electron and hole paths to the left and right of the vertical dashed line.

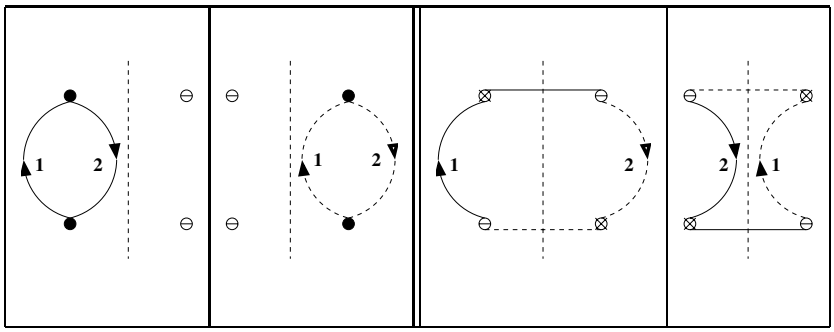

Figure 2. Lowest order diagrams, x_1, x_2, x_3 and x_4, with two scattering events at S/F interfaces.

In the S/F/S geometry, the closed loops connect both outer interfaces (even number of reflections) and $\Gamma^{(n)}$ has only even indices. Thus we can approximate the denominator expansion to lowest order with

$$\frac{1}{\Gamma^{(2)}} = 1 + x_1 + x_2 + x_3 + x_4,$$

where

$$x_1 = \tilde{b}_{eL}\tilde{b}_{eR}, \qquad x_2 = \tilde{b}_{hL}\tilde{b}_{hR}, \tag{16}$$

$$x_3 = \tilde{a}_{eR}\tilde{a}_{hL}, \qquad x_4 = \tilde{a}_{hR}\tilde{a}_{eL}, \tag{17}$$

with the tilted scattering amplitudes given by the corresponding untilted amplitudes, like $a_{p\alpha}$ defined in the appendix for an S/F interface, multiplied by the preceding propagation factor as previously. Thus the propagation factors are $e^{2iS_e}(e^{-2iS_h})$, for $x_1(x_2)$ correspondingly and $e^{i(S_e-S_h)}$ for x_3 and x_4, with $S_e(S_h)$ being the electron (hole) propagation phases. The terms x_1 and x_2 that correspond to normal reflections have no ϕ dependence, while in the Andreev processes $x_3(x_4)$ the phase enters as $e^{i\phi}(e^{-i\phi})$ correspondingly, with $\phi = \phi_R - \phi_L$ being the phase difference between the two superconductors.

The next-order expansion of the denominator is

$$\begin{aligned}\frac{1}{\Gamma^{(4)}} = {} & 1 + x_1 + x_2 + x_3 + x_4 + x_5 + x_6 + x_1^2 + x_2^2 + x_3^2 + x_4^2 + x_1x_2 + x_3x_4 \\ & + x_1x_3 + x_3x_1 + x_1x_4 + x_4x_1 + x_2x_3 + x_3x_2 + x_2x_4 + x_4x_2,\end{aligned} \tag{18}$$

where

$$x_5 = \tilde{b}_{eR}\tilde{a}_{eL}\tilde{b}_{hR}\tilde{a}_{hL}, \qquad x_6 = \tilde{a}_{eR}\tilde{b}_{hL}\tilde{a}_{hR}\tilde{b}_{eL}. \tag{19}$$

The x_5, x_6 are basic processes since they cannot be decomposed into lower order processes. The term x_1x_3 appears also as x_3x_1 because they correspond to different closed loops (see columns 2 and 3 in figure 3), which is the case for all products in (18) except x_1x_2 and x_3x_4, which involve electron and hole acting simultaneously. Thus we can rewrite (18) as

$$\begin{aligned}\frac{1}{\Gamma^{(4)}} &= 1 + x_1 + x_2 + x_3 + x_4 + x_5 + x_6 - x_1x_2 - x_3x_4 + \sum_{i,j=1}^{4} x_ix_j \\ &= 1 + \gamma + \sum_{i,j=1}^{4} x_ix_j.\end{aligned} \tag{20}$$

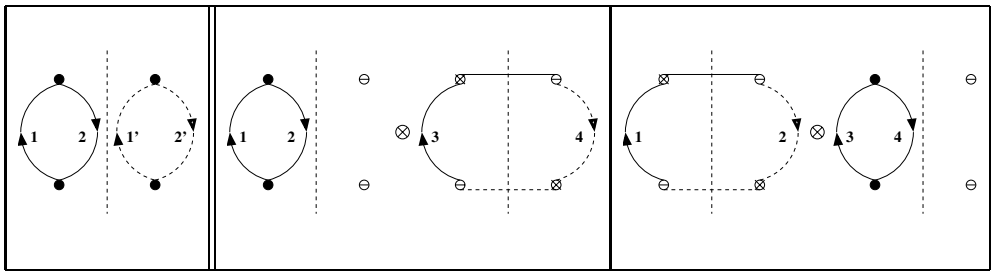

Figure 3. Processes x_1x_2, x_1x_3, x_3x_1.

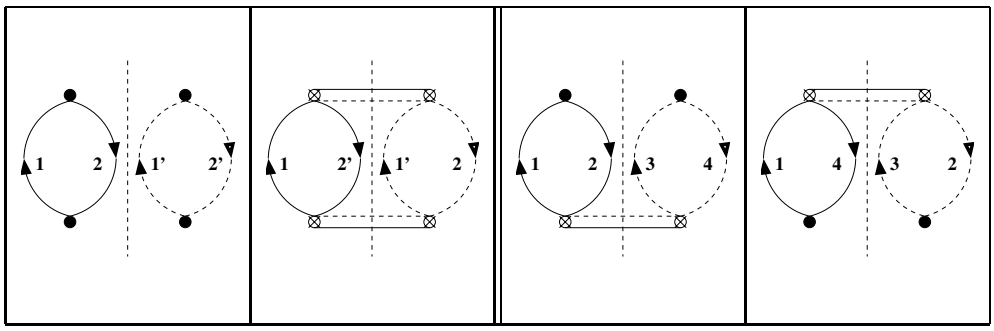

Figure 4. Processes x_1x_2, x_3x_4, x_5, x_6. The double (continuous and dashed) line denotes Andreev processes in both directions with incident electron and hole.

Defining γ in this problem as

$$\gamma = x_1 + x_2 + x_3 + x_4 - (x_1x_2 + x_3x_4 - x_5 - x_6) \equiv \gamma_2 + \gamma_4, \tag{21}$$

where the processes in γ_4 (four scattering events) x_1x_2, x_3x_4, x_5, x_6 are shown in figure 4. The full expansion of the denominator is

$$\frac{1}{\Gamma} = 1 + \gamma + \gamma^2 + \cdots = \frac{1}{1-\gamma}, \tag{22}$$

where we completed the γ^2 term by including the summation term in (20) along with higher order terms. In the appendix (see appendix A.4), we show that such a rearrangement is possible for each power of γ. These diagrams have also been shown in [23], where they are identified as first-order transport processes, when expanding the denominator.

So to calculate γ one must take into account all loops, which have at most one scattering event at each vertex at the S/F interfaces. The loops that must be taken into account and are not basic (such as x_1x_2 and x_3x_4) have a sign, which is given by $(-1)^{\nu-1}$, where ν is the number of the basic loops from which they are made up ($\nu = 2$ for these cases).

The processes in figure 4 can be summed with the appropriate signs in the form

$$\gamma_4 = -(x_1x_2 + x_3x_4 - x_5 - x_6) = g_L g_R,$$

with

$$g_\alpha = \tilde{b}_{e\alpha}\tilde{b}_{h\alpha} - \tilde{a}_{e\alpha}\tilde{a}_{h\alpha}, \qquad \alpha = L, R, \tag{23}$$

where $g_L(g_R)$ are associated with the left(right) S/F interface, and even though they do not correspond to closed loops, when taken separately, they do so when taken as the product $g_L g_R$. In that case they are the summation of four closed loops. Thus we will see that in the case of a

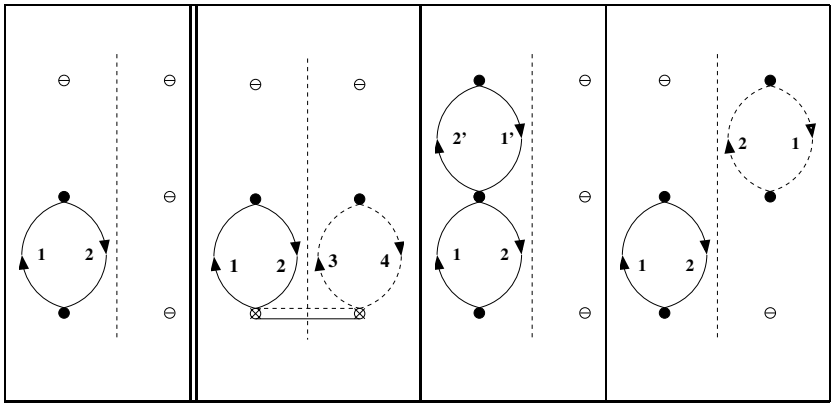

Figure 5. Examples of processes with one (column 1) and two (columns 2–4) active S/F vertices.

multilayer ferromagnet when both vertices (at electron and hole paths) at an SF interface are active, the combination that appears in Γ for the loops is $g_L(g_R)$ for the left(right) interface. Of course, they must be multiplied by the appropriate amplitudes to give closed loops. This combination gives no ϕ dependence which would arise only from Andreev reflections, but in this case is canceled because we have both processes of electron and hole Andreev reflections.

3.3. The $S_L/F_1/F_2/S_R$ *case*

Now with these tools we want to construct directly Γ for an S/F/F/S junction. This will give the possibility of substituting in the place of the F/F interface scattering amplitudes those for more complicated intermediate structures. First, we categorize the diagrams that must be taken into account by the number of S/F vertices, which are active. There are four categories according to 1, 2, 3 or 4 vertices being active, so we can write

$$\frac{1}{\Gamma} = \frac{1}{1-(\gamma_1+\gamma_2+\gamma_3+\gamma_4)}.$$

When only one vertex at an S/F interface is active (see figure 5 (column 1) for an example), the intermediate F/F vertices are single-linked, so that γ_1 is equal to

$$\gamma_1 = \sum_p \tilde{b}_{pL}\tilde{r}^p_{12} + \sum_p \tilde{b}_{pR}\left(\tilde{r}^p_{12}\right)', \tag{24}$$

with the first (second) terms involving normal reflections at $L(R)$ S/F interfaces for $p = e, h$.

The case of two active vertices has two possibilities, i.e. both active vertices are at one S/F interface (contributing g_L or g_R), or one vertex at each interface is active. Thus we have

$$\gamma_2 = -g_L\tilde{r}^e_{12}\tilde{r}^h_{12} - g_R\left(\tilde{r}^e_{12}\right)'\left(\tilde{r}^h_{12}\right)' - \sum_p \tilde{b}_{pL}\tilde{b}_{pR}g^p_{N12} - \sum_p \tilde{b}_{pL}\tilde{b}_{\bar{p}R}\tilde{r}^p_{12}\left(\tilde{r}^{\bar{p}}_{12}\right)'$$
$$+\tilde{a}_{hL}\left(\tilde{t}^h_{12}\right)'\tilde{a}_{eR}\tilde{t}^e_{12} + \tilde{a}_{eL}\left(\tilde{t}^e_{12}\right)'\tilde{a}_{hR}\tilde{t}^h_{12}, \tag{25}$$

where $\bar{p} = h, e$ correspondingly for $p = e, h$. The signs are consistent ($(-1)^{\nu-1}$) for the terms that involve products of ν basic loops.

In the first term in (25) both intermediate vertices (in the electron and hole paths) are singly linked, i.e. only to the left S/F interface (for an example, see column 2 in figure 5), while

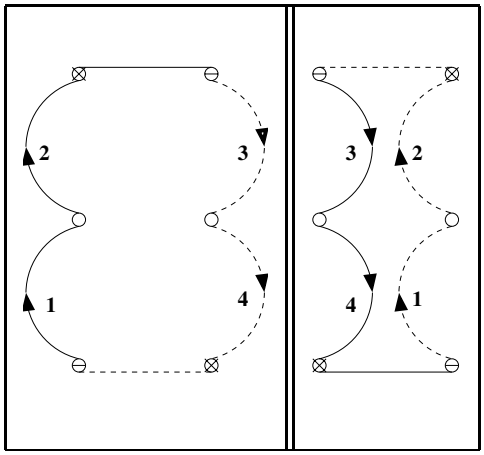

Figure 6. Andreev reflection processes with two active S/F vertices.

in the second term both intermediate vertices are singly linked with the right S/F interface. Note that g_L must be multiplied by $\tilde{r}^e_{12}\tilde{r}^h_{12}$ to form closed loops for both terms in g_L.

In the second case, one intermediate vertex is doubly linked (third term in (25)), contributing g^p_{N12} if both S/F vertices are on the same side (electron or hole paths), as in column 3 of figure 5 for the electron path, or both intermediate vertices (electron and hole) are singly linked, each with a different S/F interface and therefore involve both electron and hole paths. This corresponds to the fourth term in (25), one contribution to which is seen in column 4 in figure 5. For the last two terms in (25), as shown in the diagrams in figure 6, we have two Andreev active vertices (one on each outer interface) and these terms are that give the ϕ dependence in the denominator. In fact, it is this type of diagram that gives the ϕ dependence in the denominator also for a multilayer ferromagnet.

For three active vertices (in γ_3), one intermediate vertex is doubly linked and one singly, with an example shown in column 1 in figure 7. Thus

$$\gamma_3 = \sum_p g_L g^p_{N12} \tilde{b}_{pR} \tilde{r}^{\bar{p}}_{12} + \sum_p g_R g^p_{N12} \tilde{b}_{pL} \left(\tilde{r}^{\bar{p}}_{12}\right)'. \tag{26}$$

Finally, if four vertices are active then both intermediate vertices are doubly linked as shown in column 2 of figure 7, so that

$$\gamma_4 = -g_L g_R g^e_{N12} g^h_{N12}. \tag{27}$$

In figures 5–7, we give examples of each group of diagrams that are involved in γ_1, γ_2, γ_3, and γ_4. A careful inspection will show that to each column correspond several similar diagrams. Thus in column 1 of figure 5 we have one loop of the four that make up the γ_1 term. To the next three columns of the same figure correspond $4 + 4 + 2 = 10$ loops of γ_2. To these we must add the two loops in figure 6. In the first column of figure 7 correspond the 16 loops of γ_3 and in the second column the 16 loops of γ_4. Thus the number of terms in γ has increased significantly. Nevertheless, we have an analytic expression for the determination of Andreev bound states (instead of a determinental form), and in special cases we can easily simplify the expression from the properties of the individual interfaces. Two such cases are briefly discussed in the following.

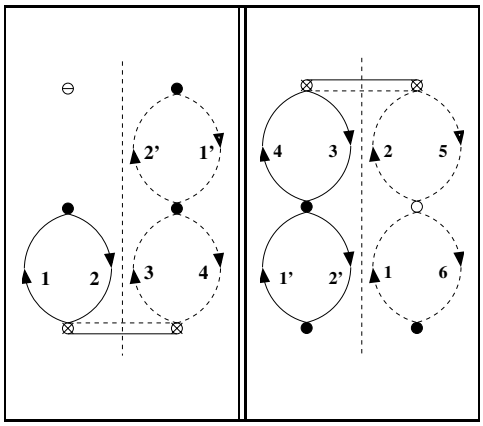

Figure 7. Examples of processes with three (column 1) and four (column 2) active S/F vertices.

3.3.1. Transparent S/F interfaces. The special case of no band misfit and transparent interfaces ($Z_L = Z_R = 0$) can be obtained in a simple analytic form if the exchange fields are weak, so that in the pre-exponential terms, i.e. in the single interface scattering amplitudes (untilted quantities in appendices A.1 and A.2), we set the normalized wavevectors equal to unity. Then the scattering amplitudes at the S/F interfaces have no normal reflections ($b_{\alpha,p} = 0$) and the Andreev amplitudes for energies in the gap are

$$a_{\alpha,p} = \frac{v}{u}\,\mathrm{e}^{\mp \mathrm{i}\phi_\alpha} = \mathrm{e}^{-\mathrm{i}\varphi_E}\,\mathrm{e}^{\mp \mathrm{i}\phi_\alpha}, \qquad \text{with} \quad \cos\varphi_E = \frac{E}{\Delta}.$$

Thus all the closed paths that contain normal reflections in the S/F interfaces are omitted and only the γ_4 and several terms from γ_2 contribute. Thus

$$\Gamma = 1 + \underbrace{g_L \tilde{r}^e_{12}\tilde{r}^h_{12} + g_R\big(\tilde{r}^e_{12}\big)'\big(\tilde{r}^h_{12}\big)' - \tilde{a}_{hL}\big(\tilde{t}^h_{12}\big)'\tilde{a}_{eR}\tilde{t}^e_{12} - \tilde{a}_{eL}\big(\tilde{t}^e_{12}\big)'\tilde{a}_{hR}\tilde{t}^h_{12}}_{-\gamma_2}$$
$$+ \underbrace{g_L g_R g^e_{N12} g^h_{N12}}_{-\gamma_4},$$

where the first two terms in γ_2 give

$$g_L\tilde{r}^e_{12}\tilde{r}^h_{12} + g_R\big(\tilde{r}^e_{12}\big)'\big(\tilde{r}^h_{12}\big)' \approx -R(\mathrm{e}^{2\mathrm{i}(q_{e1}d_1 - q_{h1}d_1 - 2\varphi_E)} + \mathrm{e}^{2\mathrm{i}(q_{e2}d_2 - q_{h2}d_2 - 2\varphi_E)}),$$

where we used

$$r^e_{12}r^h_{12} \approx \big(r^e_{12}\big)'\big(r^h_{12}\big)' \approx \frac{Z^2}{4+Z^2} \longrightarrow R,$$

with R being the reflection coefficient with no misfit. The next two terms give the ϕ dependence and sum to $-2T\mathrm{e}^{\mathrm{i}(S_e - S_h - 2\varphi_E)}\cos\phi$, where we used the transmission coefficient for the middle F/F interface (with no misfit),

$$t^e_{12}\big(t^h_{12}\big)' \approx \big(t^e_{12}\big)'t^h_{12} \approx \frac{4}{4+Z^2} \to T,$$

and $(S_e - S_h) = (q_{1e}d_1 + q_{2e}d_2) - (q_{1h}d_1 + q_{2h}d_2)$ is the propagation phase. The last term in (28) is approximated as $-\mathrm{e}^{2\mathrm{i}(S_e - S_h - 2\varphi_E)}$. Summing all terms and dividing by the coefficient of $T\cos\phi$, we get from the vanishing of Γ the condition for the Andreev bound states,

$$\cos(S_e - S_h - 2\varphi_E) = R\cos(\Delta_e - \Delta_h) + T\cos\phi,$$

where $\Delta_p = q_{p2}d_2 - q_{p1}d_1$ measures the propagation phase difference in the two layers [24, 37].

3.3.2. Double S/F interface barriers. The special case of no band misfit and transparent F/F interface ($Z_L = Z_R = Z$ and $Z_{12} = 0$) can be obtained in a simple analytic form if the exchange fields are weak, so that again in the pre-exponential terms, i.e. in the single interface scattering amplitudes (untilted quantities) we set the normalized wavevectors equal to unity. The scattering amplitudes at the S/F interfaces ($b_{\alpha,p}$ and $a_{\alpha,p}$) are given in the appendix. Of course, $r_{12}^p = \left(r_{12}^p\right)' = 0$, so that we have no contribution from γ_1 and γ_3, while we have unity transmission, i.e. $t_{12}^p = \left(t_{12}^p\right)' = 1$. The nonzero contributions from γ_2 and γ_4 give

$$\begin{aligned}\Gamma &= 1 - \sum_p \tilde{b}_{pL}\tilde{b}_{pR}\tilde{t}_{12}^p\left(\tilde{t}_{12}^{\bar{p}}\right)' - \tilde{a}_{hL}(\tilde{t}_{12}^h)'\tilde{a}_{eR}\tilde{t}_{12}^e - \tilde{a}_{eL}\left(\tilde{t}_{12}^e\right)'\tilde{a}_{hR}\tilde{t}_{12}^h + g_L g_R\left(\tilde{t}_{12}^e\right)'\tilde{t}_{12}^e\left(\tilde{t}_{12}^h\right)'\tilde{t}_{12}^h \\ &= 1 - b_e^2\,\mathrm{e}^{2\mathrm{i}S_e} - b_h^2\,\mathrm{e}^{-2\mathrm{i}S_h} - 2a_{0h}a_{0e}\cos\phi\,\mathrm{e}^{\mathrm{i}(S_e-S_h)} + (b_e b_h - a_{0h}a_{0e})^2\,\mathrm{e}^{2\mathrm{i}(S_e-S_h)}, \qquad (28)\end{aligned}$$

where the propagation phases are shown explicitly, the parameters b_e, b_h are those given in the appendix in (A.8), (A.9) and a_{0e}, a_{0h} are given in (A.7), without the phase-dependent exponential factors, i.e. $a_{0e} = a_e(\phi = 0)$. In all cases, we use the approximations in this section and one can show that at an S/F interface

$$\begin{aligned}(b_e b_h - a_h a_e) &= \frac{1}{\gamma_{SF}}[(k_e - q_e + \mathrm{i}Z)(k_h - q_h - \mathrm{i}Z)u^2 - (k_e + q_h + \mathrm{i}Z)(k_h + q_e - \mathrm{i}Z)v^2] \\ &\approx \frac{1}{\gamma_{SF}}[Z^2(u^2 - v^2) - 4v^2], \qquad (29)\end{aligned}$$

where γ_{SF} is given in (A.10) with the approximations in this section. Dividing the expression for Γ by $\frac{1}{\gamma_{SF}^2}32u^2v^2\,\mathrm{e}^{\mathrm{i}(S_e-S_h)}$ (the coefficient of $\cos\phi$) we get from $\Gamma = 0$, the equation that determines the Andreev bound states [36],

$$\begin{aligned}\cos\phi = \cos(S_e - S_h - 2\varphi_E) &- \frac{Z^4}{4}\sin^2\varphi_E\cos(S_e - S_h) + Z^2\sin\varphi_E\sin(S_e - S_h - \varphi_E) \\ &+ \frac{Z^2}{4}\sin^2\varphi_E[(Z^2 - 4)\cos(S_e + S_h) - 4Z\sin(S_e + S_h)]. \qquad (30)\end{aligned}$$

4. Multilayer ferromagnet

The above procedure can be extended to a multilayer ferromagnet. In this case, when three or more layers are included, we must consider the possibility of closed loops with no active S/F interfaces. For example, for three layers these are shown in figure 8. These loops are included in the term γ_0, which must be added to the denominator Γ. Thus in this case, Γ can be written as

$$\frac{1}{\Gamma} = \frac{1}{1 - (\gamma_0 + \gamma_1 + \gamma_2 + \gamma_3 + \gamma_4)}. \qquad (31)$$

The closed loops with no active vertices at the S/F interfaces give

$$\gamma_0 = \left(\tilde{r}_{12}^e\right)'\tilde{r}_{23}^e + \left(\tilde{r}_{12}^h\right)'\tilde{r}_{23}^h - \left(\left(\tilde{r}_{12}^e\right)'\tilde{r}_{23}^e\right)\left(\left(\tilde{r}_{12}^h\right)'\tilde{r}_{23}^h\right), \qquad (32)$$

where the last term is the product of two basic loops, leading to the minus sign. Of course, for more layers there arise a large variety of such loops, which must be included also in higher order active S/F interfaces. Care again must be taken whether the closed loop is a basic process (as defined earlier) or a compound process in order to determine the proper sign.

In this procedure, the denominator is expressed in terms of the scattering amplitudes of FS barriers ($a_{p\alpha}, b_{p\alpha}$, for $p = e, h$ and $\alpha = L, R$) and the $\mathrm{F}_i/\mathrm{F}_{i+1}$ barriers ($r_{i,i+1}, t_{i,i+1}, r'_{i,i+1}, t'_{i,i+1}$ for $i = 1, \ldots, n-1$). As an example, we explicitly work out the summation of the closed loops for the three layer ferromagnet in terms of ($r_{i,i+1}, t_{i,i+1}, r'_{i,i+1}, t'_{i,i+1}$ for $i = 1, 2$) and show

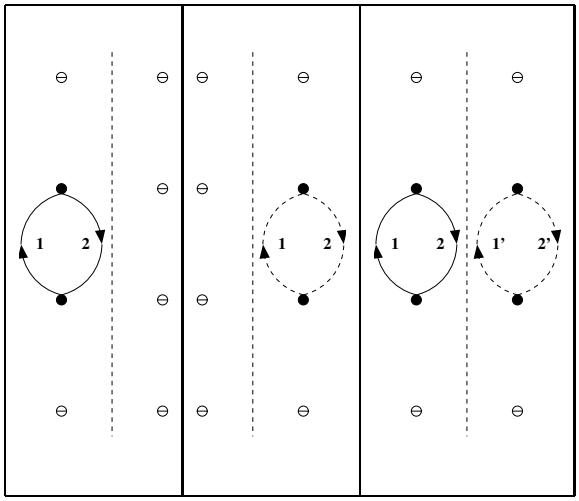

Figure 8. Closed loops that contribute to γ_0.

that it reduces to the result of the two-layer but with the $(r_{1,3}, t_{1,3}, r'_{1,3}, t'_{1,3})$ amplitudes. The details are shown in appendix 7.5, using only the diagrammatic procedure along with proper rearrangement.

The procedure can be summarized in the simple rules as follows.

(a) To calculate γ, one must take into account all loops, which have at most one scattering event at each vertex at the S/F interfaces.
(b) The loops that must be taken into account and are not basic have a sign, which is given by $(-1)^{\nu-1}$, where ν is the number of the basic loops from which they are made up.
(c) When both vertices (at electron and hole paths) at an SF interface are active, the combination that appears in Γ for the loops is $g_L(g_R)$ for the left(right) interface.
(d) With each doubly linked (to neighbors) vertex at an intermediate interface (F_i/F_{i+1}) we associate the vertex quantity $g^p_{N,i,i+1}$ for $p = e(h)$ correspondingly for the electron (hole) vertex.
(e) In any term in γ, we include closed paths with at most one loop in each ferromagnetic layer for a given particle. This allows for two loops in the same layer, only if they are one on the electron and the other on the hole paths. This rule will be used in the following.

Equivalently, we can achieve the same if we split the problem in three steps.

(a) Find Γ for an $S_L/F_1/F_n/S_R$ junction with two ferromagnetic layers, in terms of the individual interface scattering amplitudes as in the previous section.
(b) In the place of the F_1/F_n barrier, we introduce $(n-2)$ ferromagnetic layers. Then we determine iteratively the total scattering amplitudes $(r_{1,n}, t_{1,n}, r'_{1,n}, t'_{1,n})$ for the n ferromagnetic layers with the individual interface amplitudes $(r_{i,i+1}, t_{i,i+1}, r'_{i,i+1}, t'_{i,i+1}$ for $i = 1, n-1)$.
(c) Introduce the results of (b) in (a).

This approach will be followed in the calculation of the total scattering amplitude matrix in the appendix (see appendix A.6). The same quantity Γ will enter but in a more complicated way. Nevertheless, we will use that derivation for the calculation of the supercurrent toward the development of a diagrammatic procedure for the current.

5. Josephson current

The current will be calculated from Green's function approach of Furusaki and Tsukada [14], which includes both the discrete spectrum and the continuum contributions

$$I = \frac{e}{2\hbar} k_B T \sum_{\omega_n,\sigma} \frac{\Delta_L}{\Omega_{nL}} (k_{eL} + k_{hL}) \left(\frac{A_{eL}}{k_{eL}} - \frac{A_{hL}}{k_{hL}} \right), \tag{33}$$

where the sum is over the Matsubara frequencies $\omega_n = (2n+1)\pi k_B T/\hbar$ for $n = 0, \pm 1, \pm 2, \ldots$ and the expression is evaluated using the analytic continuation $E + \mathrm{i}0^+ \to \mathrm{i}\hbar\omega_n$, so that $\Omega_L \to \mathrm{i}\Omega_{nL}$. The formula takes into account the degeneracy between left-going electron and right-going hole and the same for the opposite directions, while there is also a summation over spins, since the exchange field splits the energy levels. The quantities A_{eL} and A_{hL} are the Andreev amplitudes for electron and hole correspondingly incident from the left superconductor and are given by the off-diagonal elements of the matrix $\hat{R}_{L\to R}$ in the appendix. To calculate the current from (33) we must evaluate

$$\frac{A_{eL}}{k_{eL}} - \frac{A_{hL}}{k_{hL}}. \tag{34}$$

We will evaluate this expression using the scattering amplitudes for the $S/F_1/F_n/S$ case, since it can be generalized to any number of ferrolayers by using the composition rules for t^p_{1n} and $\left(t^p_{1n}\right)'$ in appendix A.6.3. While each Andreev amplitude is a complicated expression, the combination in (33) leads to cancelations from the two terms and great simplification in the numerator of this expression. The denominator is proportional to Γ, as defined in the S/F/F/S case, taking into account the analytic continuation at the Matsubara frequencies.

After some algebraic manipulation and using the identities

$$\frac{a^*_{eL}}{k_{eL}} - \frac{a^*_{hL}}{k_{hL}} = 0 \tag{35}$$

$$d_{eL}\frac{c^*_{eL}}{k_{eL}} - c_{eL}\frac{d^*_{hL}}{k_{hL}} = 0 = c_{hL}\frac{d^*_{eL}}{k_{eL}} - d_{hL}\frac{c^*_{hL}}{k_{hL}} \tag{36}$$

$$a_{eL}\left(c_{hL}\frac{c^*_{eL}}{k_{eL}} - d_{hL}\frac{d^*_{hL}}{k_{hL}} \right) + a_{hL}\left(d_{eL}\frac{d^*_{eL}}{k_{eL}} - c_{eL}\frac{c^*_{hL}}{k_{hL}} \right) = 0, \tag{37}$$

we derive for the expression

$$\begin{aligned} \frac{A_{eL}}{k_{eL}} - \frac{A_{hL}}{k_{hL}} = {} & \tilde{a}_{eR}\tilde{t}^e_{1n}\left(\tilde{t}^h_{1n}\right)' \left(\tilde{c}_{hL}\frac{c^*_{eL}}{k_{eL}} - \tilde{d}_{hL}\frac{d^*_{hL}}{k_{hL}} \right)\frac{1}{\Gamma} \\ & + \tilde{a}_{hR}\left(\tilde{t}^e_{1n}\right)'\tilde{t}^h_{1n} \left(\tilde{d}_{eL}\frac{d^*_{eL}}{k_{eL}} - \tilde{c}_{eL}\frac{c^*_{hL}}{k_{hL}} \right)\frac{1}{\Gamma}. \end{aligned} \tag{38}$$

This expression includes the possibility of n-ferromagnetic layers, which enter through the transmission amplitudes of electrons and holes across the ferromagnetic layers to the right $\left(t^e_{1n}, t^h_{1n}\right)$, and in the opposite direction $\left(\left(t^e_{1n}\right)', \left(t^h_{1n}\right)'\right)$. The terms that contribute in (38) to first order (proportional to a_{eR} or a_{hR}) are described by the diagrams in figure 9, if we neglect the expansion of Γ.

5.1. Diagram summation for supercurrent in SFS

In the previous paragraph the current was obtained from the scattering matrix, but the same could be obtained from the diagrammatic approach. We will try to do it by examining the

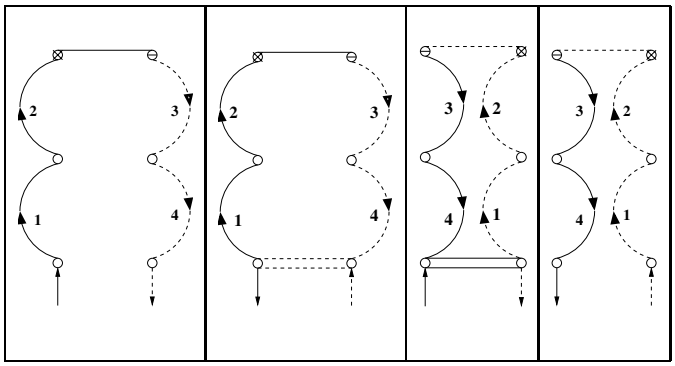

Figure 9. First-order processes that contribute to the current for the S/F/F/S structure.

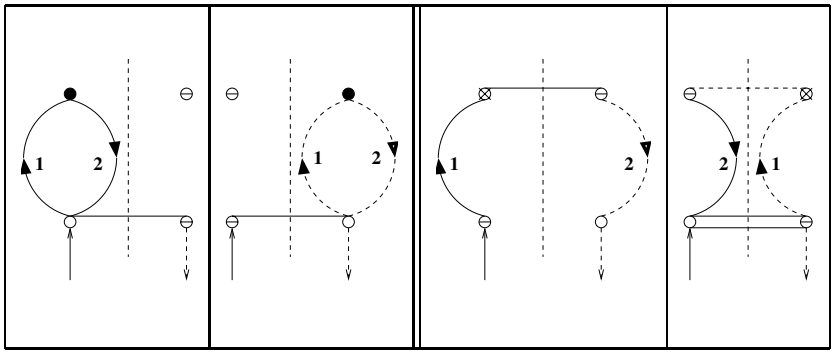

Figure 10. First-order processes, for electron-like incidence, contributing proportional to M_1, M_2, M_3, M_4.

single-ferromagnetic layer for simplicity (i.e. setting $\tilde{t}^p_{1n} = \left(\tilde{t}^p_{1n}\right)' \approx 1$ and $\tilde{r}^e_{1n} = \left(\tilde{r}^h_{1n}\right)' \approx 0$). Again we order the diagrams according to the number of interior reflections (normal or Andreev). In figure 10, we give the first-order diagrams (proportional to a_{pR} or b_{pR} with $p = e, h$) for electron-like incidence, which in terms of scattering amplitudes are

$$M_1 = \tilde{d}_{eL}\tilde{b}_{eR}\frac{c^*_{eL}}{k_{eL}} \equiv y_1\frac{c^*_{eL}}{k_{eL}}, \qquad M_3 = \tilde{c}_{hL}\tilde{a}_{eR}\frac{c^*_{eL}}{k_{eL}} \equiv y_3\frac{c^*_{eL}}{k_{eL}},$$
$$M_2 = \tilde{c}_{hL}\tilde{b}_{hR}\frac{d^*_{eL}}{k_{eL}} \equiv y_2\frac{d^*_{eL}}{k_{eL}}, \qquad M_4 = \tilde{d}_{eL}\tilde{a}_{hR}\frac{d^*_{eL}}{k_{eL}} \equiv y_4\frac{d^*_{eL}}{k_{eL}}.$$

Note that there are also zero-order diagrams with direct Andreev reflections for incident electron-like and hole-like quasiparticles, giving correspondingly contributions $\frac{a^*_{eL}}{k_{eL}}$ and $-\frac{a^*_{hL}}{k_{hL}}$ so that their sum vanishes due to (35).

In figure 11, we give the first-order diagrams (proportional to a_{pR} or b_{pR} with $p = e, h$) for hole-like incidence, which in terms of scattering amplitudes are

$$M'_1 = \tilde{c}_{eL}\tilde{b}_{eR}\frac{d^*_{hL}}{k_{hL}} \equiv y'_1\frac{d^*_{hL}}{k_{hL}}, \qquad M'_3 = \tilde{d}_{hL}\tilde{a}_{eR}\frac{d^*_{hL}}{k_{hL}} \equiv y'_3\frac{d^*_{hL}}{k_{hL}}.$$
$$M'_2 = \tilde{d}_{hL}\tilde{b}_{hR}\frac{c^*_{hL}}{k_{hL}} \equiv y'_2\frac{c^*_{hL}}{k_{hL}}, \qquad M'_4 = \tilde{c}_{eL}\tilde{a}_{hR}\frac{c^*_{hL}}{k_{hL}} \equiv y'_4\frac{c^*_{hL}}{k_{hL}}.$$

Note that from the balance conditions (36) we have $M_1 = M'_1$ and $M_2 = M'_2$.

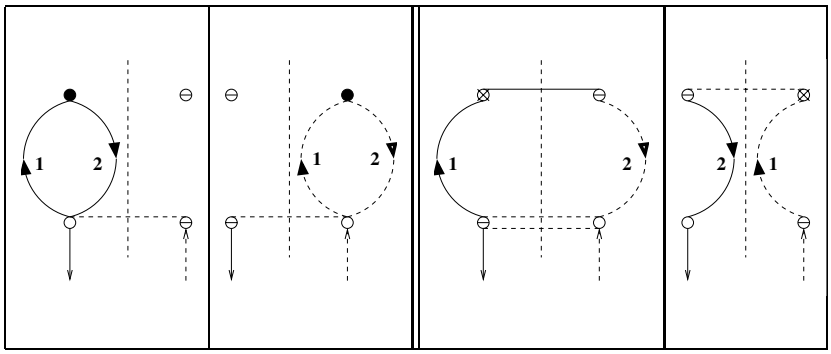

Figure 11. First-order processes, for hole-like incidence, contributing proportional to M_1', M_2', M_3', M_4'.

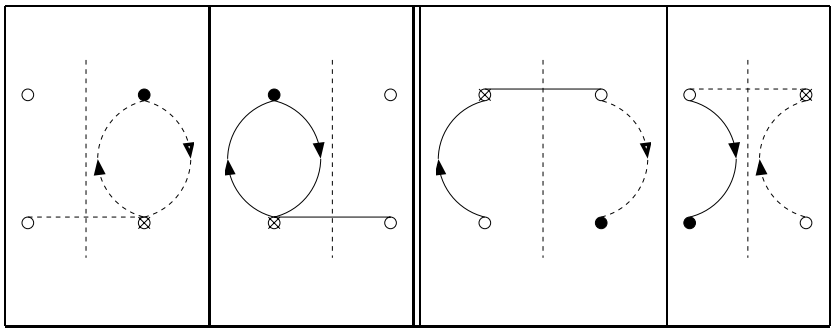

Figure 12. Auxiliary diagrams z_1, z_2, z_3, z_4.

Summation of the eight first-order diagrams above with the appropriate sign for the particles, and the balance conditions (36), gives

$$(M_1 + M_3) - (M_1' + M_3') + (M_2 + M_4) - (M_2' + M_4') = \left(\frac{c_{eL}^*}{k_{eL}} y_3 - \frac{d_{hL}^*}{k_{hL}} y_3'\right) + \left(\frac{d_{eL}^*}{k_{eL}} y_4 - \frac{c_{hL}^*}{k_{hL}} y_4'\right),$$

which is the first term in the current if one expands Γ, i.e. omitting multiple internal reflections, so that

$$I^{(1)} = \frac{e}{2\hbar} k_B T \sum_{\omega_n,\sigma} \frac{\Delta_L}{\Omega_{nL}} (k_{eL} + k_{hL}) \left[\left(\frac{c_{eL}^*}{k_{eL}} y_3 - \frac{d_{hL}^*}{k_{hL}} y_3'\right) + \left(\frac{d_{eL}^*}{k_{eL}} y_4 - \frac{c_{hL}^*}{k_{hL}} y_4'\right) \right]. \tag{39}$$

The number of the next-order (in the reflections) diagrams, which correspond to paths (not necessarily closed) that contribute to the current is 16 for electron-like incidence and 16 for hole-like incidence. Using the auxiliary functions $z_i; i = 1, 2, 3, 4$,

$$z_1 = \tilde{a}_{hL}\tilde{b}_{hR}, \qquad z_2 = \tilde{a}_{eL}\tilde{b}_{eR}, \qquad z_3 = \tilde{b}_{hL}\tilde{a}_{eR}, \qquad z_4 = \tilde{b}_{eL}\tilde{a}_{hR},$$

with the corresponding diagrams in figure 12 and the closed-loop diagrams $x_i; i = 1, 2, 3, 4$ (defined in section 3.2 where we calculate the SFS denominator) the contribution to third order

is proportional to

$$\begin{aligned} N_3 = &\frac{c^*_{eL}}{k_{eL}}((x_1+x_3)(y_1+y_3)+(z_1+z_3)(y_2+y_4)) \\ &+\frac{d^*_{eL}}{k_{eL}}((x_2+x_4)(y_2+y_4)+(z_2+z_4)(y_1+y_3)) \\ &-\frac{d^*_{hL}}{k_{hL}}((x_1+x_3)(y'_1+y'_3)+(z_1+z_3)(y'_2+y'_4)) \\ &+\frac{c^*_{hL}}{k_{hL}}((x_2+x_4)(y'_2+y'_4)+(z_2+z_4)(y'_1+y'_3)), \end{aligned}$$

which can be simplified to

$$N_3 = (x_1+x_2+x_3)\left(\frac{c^*_{eL}}{k_{eL}}y_3 - \frac{d^*_{hL}}{k_{hL}}y'_3\right) + (x_1+x_2+x_4)\left(\frac{d^*_{eL}}{k_{eL}}y_4 - \frac{c^*_{hL}}{k_{hL}}y'_4\right), \tag{40}$$

by using the balance conditions and the following identities:

$$\begin{aligned} x_2y_3 &= \tilde{b}_{hL}\tilde{b}_{hR}\tilde{a}_{eR}\tilde{c}_{hL} = z_3y_2 \\ x_2y'_3 &= \tilde{b}_{hL}\tilde{b}_{hR}\tilde{a}_{eR}\tilde{d}_{hL} = z_3y'_2 \\ x_1y_4 &= \tilde{b}_{eL}\tilde{b}_{eR}\tilde{a}_{hR}\tilde{d}_{eL} = z_4y_1 \\ x_1y'_4 &= \tilde{b}_{eL}\tilde{b}_{eR}\tilde{a}_{hR}\tilde{c}_{eL} = z_4y'_1. \end{aligned}$$

And finally using (37), the current up to third order is

$$I^{(3)} = \frac{e}{2\hbar}k_BT\sum_{\omega_n,\sigma}\frac{\Delta_L}{\Omega_{nL}}(k_{eL}+k_{hL})(1+\gamma_2)\left[\left(\frac{c^*_{eL}}{k_{eL}}y_3 - \frac{d^*_{hL}}{k_{hL}}y'_3\right)+\left(\frac{d^*_{eL}}{k_{eL}}y_4 - \frac{c^*_{hL}}{k_{hL}}y'_4\right)\right], \tag{41}$$

where $\gamma_2 = (x_1+x_2+x_3+x_4)$ is defined earlier in the S/F/S case.

One could sum all the orders as for the determination of the closed loops in the bound states to obtain consecutively from the diagram summation

$$\begin{aligned} &(1+\gamma+\gamma^2+\cdots)\left(\frac{c^*_{eL}}{k_{eL}}y_3 - \frac{d^*_{hL}}{k_{hL}}y'_4 + \frac{d^*_{eL}}{k_{eL}}y_4 - \frac{c^*_{hL}}{k_{hL}}y'_3\right) \\ &\quad\equiv \frac{1}{1-\gamma}\left(\frac{c^*_{eL}}{k_{eL}}y_3 - \frac{d^*_{hL}}{k_{hL}}y'_4 + \frac{d^*_{eL}}{k_{eL}}y_4 - \frac{c^*_{hL}}{k_{hL}}y'_3\right), \end{aligned} \tag{42}$$

with γ given in (21). The same result is obtained from the scattering matrix method in (33). We should also note that some of the diagrams in N_3 are open but they cancel out and do not contribute to the current expression.

Finally, combining (33), (42) and the expressions in the appendix for the S_L/F interface parameters we find the expression

$$I = \frac{e}{2\hbar}k_BT\sum_{\omega_n,\sigma}\frac{4D}{\Gamma\gamma_L\gamma_R}\,\mathrm{e}^{\mathrm{i}(q_e-q_h)d}\sin\phi, \tag{43}$$

with

$$D = -2(2\mathrm{i}q_e)(2\mathrm{i}q_h)(k_{eL}+k_{hL})(k_{eR}+k_{hR})u_Lv_Lu_Rv_R,$$

and all the quantities are expressed in the Matsubara frequencies with the analytic continuation $E+\mathrm{i}0^+ \to \mathrm{i}\hbar\omega_n$. Γ for the S/F/S structure is given by (22), (21) and the γ_L and γ_R are the denominators in the scattering amplitudes given in (A.10).

To demonstrate the usefulness of the diagrammatic approach we consider the following two cases: (i) strong interface scattering in SIFIS and (ii) of perfect interface between the left superconductor and the ferromagnet (SFIS).

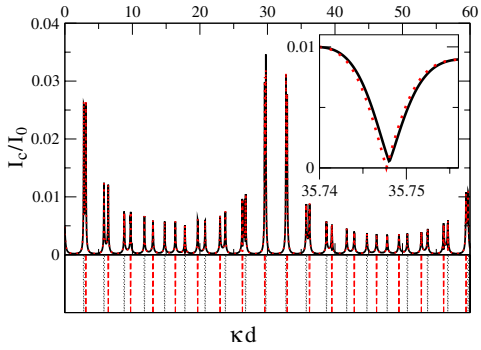

Figure 13. Normalized critical current versus κd for $Z = 10$, $h = 0.1$. Solid curve is the result of the full diagrammatic contribution, while the dotted line is the approximation $\Gamma \approx (1-x_1)(1-x_2)$. The other parameters are chosen $t = T/T_c = 0.1$.

5.2. Resonance for strong interface scattering

The case of strong interface potentials [38] (taken equal, i.e. $Z_L = Z_R = Z$) means that the normal reflection processes are important, so that the denominator can be approximated by

$$\Gamma \approx 1 - x_1 - x_2 + x_1 x_2 = (1 - x_1)(1 - x_2).$$

This means that for not very strong exchange field, the resonances due to the potential well will dominate the critical current. Thus in figure 13 we show the critical current (absolute value) as a function of the ferromagnet width κd, and we see a series of peaks, whose separation varies periodically. Across each peak there is a transition from 0-to-π junction [38], or vice versa, so that between the peaks we have the 0-junction and on either side π-junction behavior. The width in d of 0 (or π) junction varies roughly with a period determined by $S_e - S_h = \pi$. Thus the envelope has the same periodicity as the $Z = 0$ case for the same exchange field. In the lower part of the figure, we plot separately $Re(1 - x_1)$ (dotted line) and $Re(1 - x_2)$ (dashed line) at $E = 0$ for one spin channel, and we see for both curves a series of sharp dips within 10^{-4} above zero at the minimum, at which the imaginary part also vanishes. Thus each time a normal resonance of either particle with spin up or spin down approaches the Fermi level, we have the triggering of the transition and we get a structured peak in the current [34, 38]. Note that if x_1 is for a spin-up electron, then x_2 is for a spin-down hole. The resonances for electron and hole of the same spin essentially coincide. In the figure, the shift comes mainly from the spin and not from the type of particle since $h \gg \Delta/E_F$. On top of this we see that the coincidence of spin-up and spin-down (electron and hole) normal resonances leads to a significant increase of the peaks. In the same figure, we compare the full result with the approximation $\Gamma = 1 - x_1 - x_2 + x_1 x_2 = (1 - x_1)(1 - x_2)$, and we see that the two curves are indistinguishable within the scale of that figure. This seems to be the case, except near the peaks, where it is necessary to include the terms $-x_3 - x_4$ in the denominator as seen in the inset, while the other terms make no important difference. In fact at the peak we have a sharp dip at the point of transition. In the approximation (without x_3 and x_4) the transition is direct (see dotted line in inset) without a second harmonic contribution, which exists in the full denominator [19], even though the overall fitting of the critical current is quite good. The terms $-x_3 - x_4$ are necessary only near the transition.

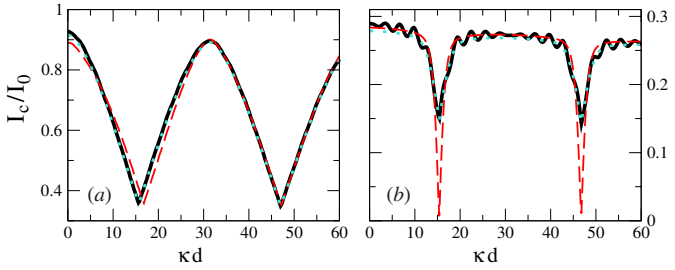

Figure 14. Normalized critical current versus κd for $Z_R = 0.1$ (a), 2.0 (b) for $h = 0.1$. Solid curve is the result of the full diagrammatic contribution, while the dashed and dotted lines are the approximations discussed in the text. The other parameters are chosen $t = T/T_c = 0.1$. Here d is unnormalized length.

5.3. The S/F/I/S case

To see the effect of misfit due to the exchange field we also consider a normal metal ($h = 0$) in the place of the ferromagnet (S/N/I/S). Even in the ferromagnet interlayer, for weak exchange field but strong right interface scattering ($Z_R \gg 1$) we can simplify the current expression. In this case we have weak normal reflections (b_{pL}) and strong Andreev reflection (a_{pL}) at the left interface, while at the right interface we have strong normal reflection (b_{pR}) and weak Andreev reflection (a_{pR}). This means that the only significant term in the denominator Γ is x_5 which is of order unity and can be approximated as

$$x_5 \approx \tilde{a}_{eL}\tilde{a}_{hL} \to \frac{v_L}{u_L}\,\mathrm{e}^{2\mathrm{i}(q_e - q_h)d}.$$

The disadvantage of this approximation is that the contribution from the discrete spectrum is very small, so that the critical current $I_c \sim \sin\phi$, which is a result expected for strong scattering. To improve this, one can also keep the processes x_3 and x_4 which give the $\cos\phi$ dependence in the denominator and some weak asymmetry. For strong $Z_R > 2$, we can obtain a simplified expression for the current by keeping only the x_5 term in the denominator,

$$I = \frac{e}{2\hbar}k_B T \sum_{\omega_n,\sigma} \frac{8\Delta^2 \sin\phi}{Z_R^2\left[\Omega_n^2 \cosh\left[\left(\frac{\hbar\omega_n}{E_F} - \mathrm{i}h\sigma\right)\kappa d\right] + \Omega_n \hbar\omega_n \sinh\left[\left(\frac{\hbar\omega_n}{E_F} - \mathrm{i}h\sigma\right)\kappa d\right]\right]}. \tag{44}$$

This expression is valid everywhere except in the transition from 0-to-π junction or vice versa.

The other limit is when also the right interface is reflectionless ($Z_R \to 0$). Then all normal reflections and branch crossing amplitudes vanish and the denominator becomes

$$\Gamma \approx 1 - (x_3 + x_4) + x_3 x_4.$$

In this case, we expect a stronger departure from the $\sin\phi$ dependence of the current.

We verify the above in figure 14 where we plot the critical current as a function of $d\kappa$. On the left of diagram $Z = 0.1$ and on the right $Z = 2$. In both cases the continuous line is the result of the full diagrammatic contribution. The dashed line in the left ($Z = 0.1$) is the approximation $\Gamma \approx 1 - (x_3 + x_4) + x_3 x_4$, which is quite close, while the addition of the x_5 term (dotted line) coincides exactly with the exact result, implying that the normal reflection terms are not significant for weak Z and h. On the left for stronger $Z = 2.0$, the dashed curve is the approximation $\Gamma \approx 1 - x_5$, while the addition of the terms x_3, x_4 (dotted line) coincides with the continuous line, except for the small amplitude oscillations at the top, which are due to normal reflections with the period $\pi/(q_e + q_h)$. In both plots, we observe the minima at the same $d\kappa$ values, determined by h, so that they correspond to $S_e - S_h = \pi/2, 3\pi/2 \ldots$,

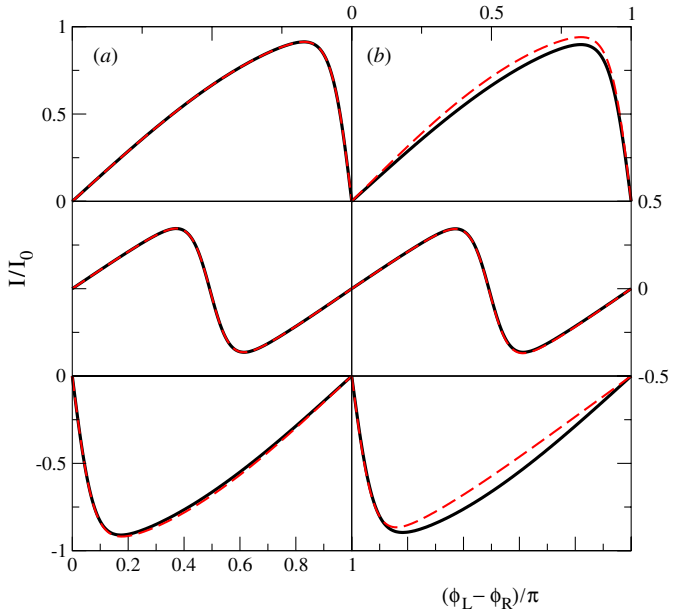

Figure 15. Normalized critical current versus $\phi_L - \phi_R$ for $Z_R = 0$ (a), 0.1 (b) for $h = 0$ (upper), 0.05 (middle), 0.1 (lower). Solid curve is the result of the full diagrammatic contribution, while the dashed line is the approximation $\Gamma \approx 1 - (x_3 + x_4) + x_3 x_4$. The other parameters are chosen $t = T/T_c = 0.1, d = 0.05$ in units of ξ_0.

i.e. to the transition points from 0-to-π junction. The dips are stronger and narrower for increasing Z.

We check the above approximations also on the $I(\phi)$ curves in the following two figures. In figure 15 for small $Z_R = 0.1$ the approximation $\Gamma \approx 1-(x_3+x_4)+x_3x_4$, gives $I(\phi)$ (dotted line) for $Z = 0, 0.1$, which is close to the exact result (full line). The result with the addition of the x_5 term coincides with that of the full denominator. The values of the exchange energy are chosen, so that $S_e - S_h = 0$ (top), $\pi/2$ (middle), π (bottom) and as expected $I(\phi)$ for the top curve corresponds to 0 junction, the bottom to π junction and the middle to the transition point.

In figure 16, where we see that for $Z_R > 2$ the x_5 term is sufficient in top ($h = 0$) and bottom ($h = 0.1$) figure, which correspond to 0 and π junctions. The addition of the terms x_3, x_4 in the dotted line is a small correction except in the middle figure where the exchange field corresponds to the 0-to-π transition point. The three values chosen for the exchange field correspond to a propagation phase $S_e - S_h = (q_e - q_h)\kappa d \approx 0, \pi, \frac{3\pi}{2}$. The terms x_1, x_2, and x_6 which involve normal reflections at both interfaces give no important changes for the whole range of Z_R values. Of course as h, or Z_R increases the interface scattering becomes more significant, so that at high h the terms x_1, x_2, x_1x_2 and x_6 should be taken into account. To decide on this, one can look at the variation of the scattering amplitudes with h and Z_R.

6. Summary

In this paper we developed a diagrammatic approach that is particularly suited to evaluate the Andreev spectrum and the supercurrent in a multiferromagnetic S/F...F/S structure. The spectrum can be derived as usual from the vanishing of the common denominator of the

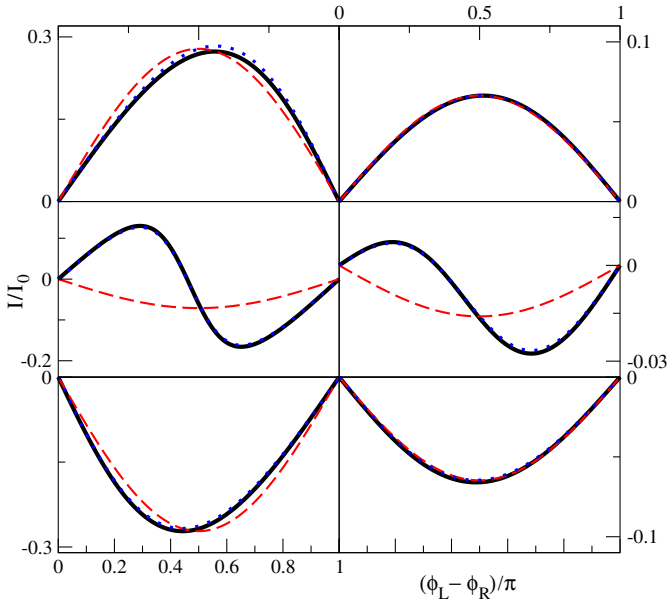

Figure 16. Normalized critical current versus $\phi_L - \phi_R$ for $Z_R = 2$ (a), 5 (b) for $h = 0$ (upper), 0.1 (middle), 0.15 (lower). Solid curve is the result of the full diagrammatic contribution, while the dashed line is the approximation $\Gamma \approx 1 - x_5$ and the dotted line also includes the contribution of ϕ-dependent terms. The other parameters are as in previous figure.

scattering amplitudes of the whole structure, which includes all the basic closed paths in the internal layers between the two S/F interfaces. By the summation of all closed processes we obtain the denominator, where only a small number of diagrams contribute, which however increases with the number of ferromagnetic layers. In the end, we obtain a set of rules for the direct construction of the condition for the bound states, using the scattering amplitudes for each interface. This gives the possibility of deciding which are the dominant paths. The approach can consider not only an inhomogeneous exchange field but also band mismatch, and the relevant information is included in the interface scattering amplitudes. In fact, one can include more general intermediate structures for which we can obtain the corresponding scattering amplitudes.

We explicitly presented the method in several steps to demonstrate and clarify the procedure. Thus we started from the trivial N/N/N/N junction, which guided us to introduce the notion of basic and not basic electron (or hole) diagrams in order to sum them properly. There we defined the vertex function g_N^p at intermediate interfaces, which is useful to group diagrams and arises again in the following structures. Next we treated consecutively the cases SIFIS, SIFIFIS, SIFIFIFIS using only diagrammatic arguments. In the last geometry (in the appendix) by rearranging the different terms and with the help of auxiliary vertex or interface functions we checked the procedure by the reduction $IFI \rightarrow I$, i.e. we wrote the three-layer denominator in the form of the two-layer but substituting the scattering amplitudes for the structure IFI instead of I in the center. Of course, this is to be expected in a scattering matrix approach and we consider it not only as a check but also as an indication of the versatility of the method. Of course, we also checked the denominator with the one obtained from the corresponding determinants in the scattering matrix. But we must stress that in our case it is not necessary to evaluate the scattering matrix. From the Andreev amplitude of the whole structure we obtain the supercurrent, for which we show the consistency of our diagrammatic

procedure. The supercurrent can be expressed with only four diagrams plus the ones that enter the denominator.

The advantage of our procedure is that it is direct and covers a general case. Also one can make the approximations in a systematic way. This was demonstrated in the two special cases treated, i.e. the strongly asymmetric SFIS, which is a structure of experimental interest and the resonant SIFIS with strong barriers. In the first example, we saw that for strong Z_R only one path contribution (x_5) is important. The possibility of 0 or π junction depends mainly on the exchange field and not on the strength of the right interface scattering. The approximation only with x_5 is quite accurate for both the Andreev spectrum and the supercurrent. It fails only near the $0 \to \pi$ transition, where it is necessary to introduce the Andreev processes x_3 and x_4. For weak interface Z_R, it is the closed Andreev paths that are more important, which also give asymmetry to the $I_c(\phi)$ curve. For the strong double barrier we reproduce earlier results and demonstrate that the important diagrams are the normal scattering closed paths obtaining a very simple expression. A fitting of the critical current is excellent except near the 0-to-π transition, where we must also include the multiple Andreev reflections, which even though they are weak they change qualitatively the behavior near the transition.

Thus there is a direct correspondence between the important physical effects and specific basic diagrams. This leads not only to improvement of speed in numerical calculations, but also to proper interpretation of the interplay of different scattering effects [5, 23]. Thus the effect of interface normal scattering in the Andreev spectrum is more than the intermixing of two normal reflections in the Andreev cycle for ideal S/F interfaces, like x_3x_2. While such processes arise from the expansion in the denominator they do not arise in the condition for the bound states.

One of the goals of future work is to examine whether there are significant band-like effects in a multilayer junction in the case of narrow resonances. For weak transmission one expects resonances to form bands. Such band structure effects have been observed experimentally in the I–V characteristics of SINININIS-type junctions [39]. Of course, here we are interested in the supercurrent enhancement through resonance coincidence. Also the diagrammatic approach is easily extended to take into account 3D junctions. There the interest will be to examine whether the phase-coherence survives for multilayers.

Appendix

A.1. Scattering amplitudes of the F/F interface

For the amplitudes from an F_i/F_{i+1} interface we use the notation where i corresponds to the left and $i+1$ to the right ferromagnet, while the unprimed (primed) are for incidence from the left (right) ferromagnet, and we have

$$r^p_{i,i+1} = \frac{q_{pi} - q_{p,i+1} \mp \mathrm{i}Z_{i,i+1}}{q_{pi} + q_{p,i+1} \pm \mathrm{i}Z_{i,i+1}}, \tag{A.1}$$

$$t^p_{i,i+1} = \frac{2q_{pi}}{q_{pi} + q_{p,i+1} \pm \mathrm{i}Z_{i,i+1}}, \tag{A.2}$$

$$\left(r^p_{i,i+1}\right)' = \frac{q_{p,i+1} - q_{pi} \mp \mathrm{i}Z_{i,i+1}}{q_{pi} + q_{p,i+1} \pm \mathrm{i}Z_{i,i+1}}, \tag{A.3}$$

$$\left(t^p_{i,i+1}\right)' = \frac{2q_{p,i+1}}{q_{pi} + q_{p,i+1} \pm \mathrm{i}Z_{i,i+1}} \tag{A.4}$$

as shown in figure 17.

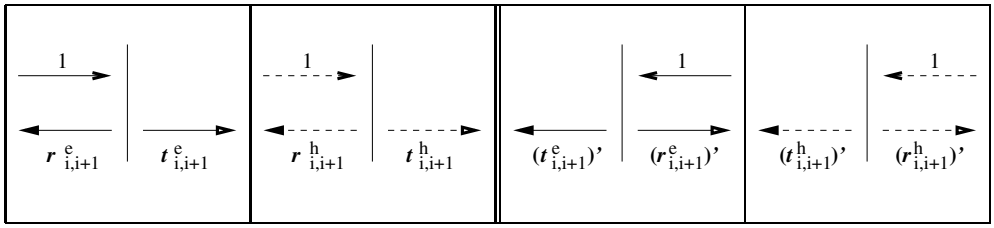

Figure 17. Definition of the scattering amplitudes for the F/F interfaces. Primed quantities correspond for incidence from the right of the interface.

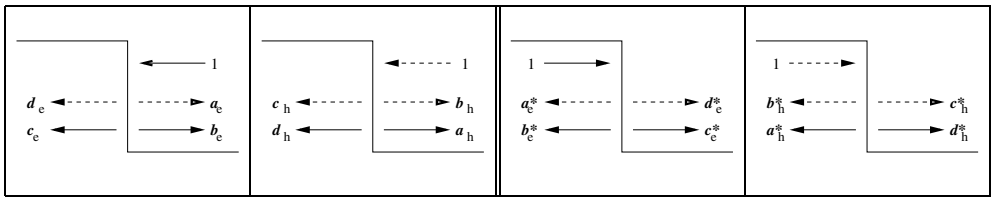

Figure 18. Definition of the scattering amplitudes at the left S/F interface. The same holds for the right S/F interface, with the starred amplitudes again corresponding for incidence from the superconductor side.

A.1.1. Scattering matrix at an F_i/F_{i+1} *interface.* For an interface (barrier strength Z_i) between two neighboring non-superconducting regions i and $i+1$ the outgoing particles are related to the incoming as follows:

$$\begin{pmatrix} \chi_{i,-e} \\ \chi_{i,-h} \\ \chi_{i+1,+e} \\ \chi_{i+1+h} \end{pmatrix} = \left(\begin{array}{cc|cc} r^e_{i,i+1} & & \left(t^e_{i,i+1}\right)' & \\ & r^h_{i,i+1} & & \left(t^h_{i,i+1}\right)' \\ \hline t^e_{i,i+1} & & \left(r^e_{i,i+1}\right)' & \\ & t^h_{i,i+1} & & \left(r^h_{i,i+1}\right)' \end{array}\right) \begin{pmatrix} \chi_{i,+e} \\ \chi_{i,+h} \\ \chi_{i+1,-e} \\ \chi_{i+1,-h} \end{pmatrix}, \tag{A.5}$$

which, using the spinor notation can be written as

$$\begin{pmatrix} \chi_{i-} \\ \chi_{(i+1)+} \end{pmatrix} = \left(\begin{array}{c|c} \hat{r}_{i,i+1} & \hat{t}'_{i,i+1} \\ \hline \hat{t}_{i,i+1} & \hat{r}'_{i,i+1} \end{array}\right) \begin{pmatrix} \chi_{i+} \\ \chi_{(i+1)-} \end{pmatrix}, \tag{A.6}$$

where $\hat{r}_{i,i+1}, \hat{r}'_{i,i+1}$ are 2×2 reflection matrices and $\hat{t}_{i,i+1}, \hat{t}'_{i,i+1}$ 2×2 transmission matrices and the prime stands for incidence from the right-hand side of the interface. The subscripts $\pm p$ denote right- or left-going p-particle.

A.2. Scattering amplitudes of the S/F interface

The analytical expressions for the scattering amplitudes from the S/F interfaces, are given below and shown in figure 18. We use the convention that the unstared elements are for incidence from the ferromagnet side and the stared (nothing to do with complex conjugation) from the superconductor side. The two superconductors are indexed with $\alpha = L, R$ and the corresponding neighboring ferromagnet with $i = 1, n$, in the case of n-ferromagnetic layers. The Andreev ($a_{p\alpha}$) and normal reflection ($b_{p\alpha}$) amplitudes for $p = e, h$-particle incidence from the ferromagnet side are

$$a_{p\alpha} = \frac{2(k_{e\alpha} + k_{h\alpha})q_{pi}u_\alpha v_\alpha}{\gamma_\alpha} \mathrm{e}^{\mp \mathrm{i}\phi_\alpha} \equiv a_{0p\alpha}\, \mathrm{e}^{\mp \mathrm{i}\phi_\alpha} \qquad \text{for} \quad p = e, h, \tag{A.7}$$

where in the exponential $e^{\mp i\phi_\alpha}$, the sign is '$-$' (+) for incident electron (hole), with $\phi_\alpha = \mp\phi/2$ ($\alpha = L, R$),

$$b_{e\alpha} = -\frac{(k_{h\alpha} + q_{hi} - iZ_\alpha)(k_{e\alpha} - q_{ei} + iZ_\alpha)u_\alpha^2 - (k_{e\alpha} - q_{hi} + iZ_\alpha)(k_{h\alpha} + q_{ei} - iZ_\alpha)v_\alpha^2}{\gamma_\alpha}, \tag{A.8}$$

$$b_{h\alpha} = -\frac{(k_{h\alpha} - q_{hi} - iZ_\alpha)(k_{e\alpha} + q_{ei} + iZ_\alpha)u_\alpha^2 - (k_{e\alpha} + q_{hi} + iZ_\alpha)(k_{h\alpha} - q_{ei} - iZ_\alpha)v_\alpha^2}{\gamma_\alpha}, \tag{A.9}$$

where we omitted the spin index from the wavevectors, but we should keep in mind that the electron and the hole have opposite spins, and the amplitudes depend on the spin. The denominator is given by

$$\gamma_\alpha = (k_{h\alpha} + q_{hi} - iZ_\alpha)(k_{e\alpha} + q_{ei} + iZ_\alpha)u_\alpha^2 - (k_{e\alpha} - q_{hi} + iZ_\alpha)(k_{h\alpha} - q_{ei} - iZ_\alpha)v_\alpha^2. \tag{A.10}$$

Furthermore, we need the normal ($c_{p\alpha}$) and branch crossing ($d_{p\alpha}$) transmission amplitudes. They are

$$c_{p\alpha} = \frac{2q_{pi}u_\alpha(k_{\bar{p}\alpha} + q_{\bar{p}i} \mp iZ_\alpha)}{\gamma_\alpha} e^{\mp i\phi_\alpha/2}, \tag{A.11}$$

$$d_{p\alpha} = \frac{2q_{pi}v_\alpha(k_{p\alpha} - q_{\bar{p}i} \pm iZ_\alpha)}{\gamma_\alpha} e^{\mp i\phi_\alpha/2}. \tag{A.12}$$

Finally, the stared coefficients for incidence from the superconductor side are

$$a^*_{p\alpha} = \frac{-2(q_{ei} + q_{hi})k_{p\alpha}u_\alpha v_\alpha}{\gamma_\alpha}, \tag{A.13}$$

$$b^*_{e\alpha} = \frac{(k_{h\alpha} + q_{hi} - iZ_\alpha)(k_{e\alpha} - q_{ei} - iZ_\alpha)u_\alpha^2 - (k_{e\alpha} + q_{hi} - iZ_\alpha)(k_{h\alpha} - q_{ei} - iZ_\alpha)v_\alpha^2}{\gamma_\alpha}, \tag{A.14}$$

$$b^*_{h\alpha} = \frac{(k_{h\alpha} - q_{hi} + iZ_\alpha)(k_{e\alpha} + q_{ei} + iZ_\alpha)u_\alpha^2 - (k_{e\alpha} - q_{hi} + iZ_\alpha)(k_{h\alpha} + q_{ei} + iZ_\alpha)v_\alpha^2}{\gamma_\alpha}, \tag{A.15}$$

$$c^*_{p\alpha} = \frac{2k_{p\alpha}u_\alpha\left(u_\alpha^2 - v_\alpha^2\right)(k_{\bar{p}\alpha} + q_{\bar{p}i} \mp iZ_\alpha)}{\gamma_\alpha} e^{\pm i\phi_\alpha/2}, \tag{A.16}$$

$$d^*_{p\alpha} = \frac{2k_{p\alpha}v_\alpha\left(u_\alpha^2 - v_\alpha^2\right)(k_{\bar{p}\alpha} - q_{pi} \mp iZ_\alpha)}{\gamma_\alpha} e^{\mp i\phi_\alpha/2}. \tag{A.17}$$

A.2.1. Scattering matrix for the right F/S interface. First we express the outgoing particles at each side of an interface with respect to the incoming particles. In a compact matrix form, for an FS interface, this yields

$$\begin{pmatrix} \chi^N_{-e} \\ \chi^N_{-h} \\ \hline \psi^S_{+e} \\ \psi^S_{+h} \end{pmatrix} = \left(\begin{array}{cc|cc} b_e & a_h & c^*_e & d^*_h \\ a_e & b_h & d^*_e & c^*_h \\ \hline c_e & d_h & b^*_e & a^*_h \\ d_e & c_h & a^*_e & b^*_h \end{array}\right) \begin{pmatrix} \chi^N_{+e} \\ \chi^N_{+h} \\ \hline \psi^S_{-e} \\ \psi^S_{-h} \end{pmatrix}, \tag{A.18}$$

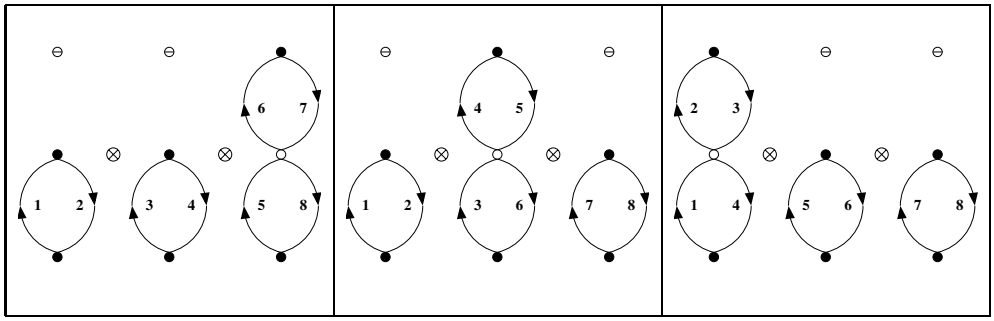

Figure 19. Processes which correspond to $x_{N1}^2 x_{N3}$.

where the subscript +(−) stands for right(left) going particles, $e(h)$ for electrons (holes) in the non-superconducting region, which are characterized by the wavefunctions χ^N, or for electron (hole)-like quasiparticles for the superconducting region, characterized by the wavefunctions ψ^S. Introducing the two-dimensional spinors $\chi_{\pm}^N$ and $\psi_{\pm}^S$, the 2×2 reflection matrices ($\hat{R}$, $\hat{R}^*$) and transmission matrices ($\hat{T}$, $\hat{T}^*$) the previous equation can be written as

$$\begin{pmatrix} \chi_-^N \\ \psi_+^S \end{pmatrix} = \left(\begin{array}{c|c} \hat{R} & \hat{T}^* \\ \hline \hat{T} & \hat{R}^* \end{array}\right) \begin{pmatrix} \chi_+^N \\ \psi_-^S \end{pmatrix}, \tag{A.19}$$

where the unstared matrices connect the outgoing particles at each side with incoming particles from the non-superconducting side and the stared with incoming quasiparticles from the superconducting side.

A.3. The enumeration of diagrams for the $N_L/N_1/N_2/N_R$ case

The choice for the closed diagrams that contribute in γ in (12) was done by considering only the second-order expansion $\frac{1}{\Gamma^{(2)}}$ in the reflection amplitudes at the outer interfaces. One must consider higher order terms in $\tilde{r}'_{L1}$ and/or $\tilde{r}_{2R}$. A general nth-order term in the expansion $\frac{1}{\Gamma^{(n)}}$ has the following form:

$$c_{m_1,m_2,m_3} x_{N1}^{m_1} x_{N2}^{m_2} x_{N3}^{m_3}, \tag{A.20}$$

where $n = m_1 + m_2 + 2m_3$ is the total number of reflections at the outer interfaces (with $n_l = m_1 + m_3$ from the left and $n_r = m_2 + m_3$ from the right) and c_{m_1,m_2,m_3} is the number of the different diagrams, which give the same contribution, i.e. the same product of scattering amplitudes and will be determined below by simple combinatorics. This number must be distributed in order to complete powers of γ in (13). The proper decomposition will be verified below.

Consider for example the term $c_{2,0,1} x_{N1}^2 x_{N3}$. As shown in figure 19 there are three different diagrams which give the same contribution $\left(x_{N1}^2 x_{N3}\right)$, where permutations between same basic diagrams are not considered. This number ($c_{2,0,1}$) is given by the combination of the reflection events from the left-hand side at the intermediate interface (N_1/N_2) out of the total events (reflection plus transmission) from the left-hand side at the intermediate interface, i.e. by the binomial

$$c_{2,0,1} = \binom{2+1}{2}. \tag{A.21}$$

If we express x_{N1}, x_{N2} and x_{N3} in terms of scattering amplitudes, then the total number of scattering events at N_1/N_2 is given by the sum of the exponents of $\tilde{r}_{12}$ and $\tilde{t}_{12}$ and the number

of reflections from the exponent of $\tilde{r}_{12}$. Thus for a general term of the form $x_{N1}^{m_1}x_{N3}^{m_3}$ the number of different diagrams is given by

$$c_{m_1,0,m_3} = \binom{m_1+m_3}{m_1}. \tag{A.22}$$

Now if reflections take place only from the right side at the intermediate interface ($m_1 = 0$ and $m_2 \neq 0$) which means that we examine terms of the form $x_{N2}^{m_2}x_{N3}^{m_3}$ the number of different diagrams is given by

$$c_{0,m_2,m_3} = \binom{m_2+m_3}{m_2}. \tag{A.23}$$

Combining the two, for the general term $x_{N1}^{m_1}x_{N2}^{m_2}x_{N3}^{m_3}$, the number of different diagrams is given by

$$c_{m_1,m_2,m_3} = \binom{m_1+m_3}{m_1}\binom{m_2+m_3}{m_2}. \tag{A.24}$$

We must compare this result with the one obtained from the expansion in powers of γ, using the multinomial expansions of the powers of γ in terms of the set of functions $(x_{N1}, x_{N2}, x_{N1}x_{N2}, x_{N3})$ and collection of the equivalent terms as $x_{N1}^{m_1}x_{N2}^{m_2}x_{N3}^{m_3}$. Consider for example the term $x_{N1}^2x_{N2}x_{N3}$. This term has contributions from the 3rd power of γ as $x_{N1}^1x_{N2}^0(x_{N1}x_{N2})^1x_{N3}^1$ and the 4th power of γ as $x_{N1}^2x_{N2}^1(x_{N1}x_{N2})^0x_{N3}^1$. Thus, in general, defining $m_0 = \min(m_1, m_2)$ and $\bar{m}_0 = \max(m_1, m_2)$ the total coefficient of a general term $x_{N1}^{m_1}x_{N2}^{m_2}x_{N3}^{m_3}$ is given by the sum

$$\sum_{i=0}^{m_0}(-1)^{m_0-i}\frac{(\bar{m}_0+i+m_3)!}{(\bar{m}_0-m_0+i)!i!(m_0-i)!m_3!}, \tag{A.25}$$

where the summation over i arises because we can combine x_{N1} and x_{N2} to make $x_{N1}x_{N2}$ factors or vice versa. The sign is determined from the sign of powers of $x_{N1}x_{N2}$.

Thus we must have

$$\sum_{i=0}^{m_0}(-1)^{m_0-i}\frac{(\bar{m}_0+i+m_3)!}{(\bar{m}_0-m_0+i)!i!(m_0-i)!m_3!} = \binom{m_1+m_3}{m_1}\binom{m_2+m_3}{m_2}, \tag{A.26}$$

which has also been checked numerically. Thus the general term $x_{N1}^{m_1}x_{N2}^{m_2}x_{N3}^{m_3}$ can be distributed appropriately so that we get the proper contribution to complete each higher power of γ, justifying the terms that contribute to γ, in (12).

A.4. The enumeration of diagrams for the $S_L/F/S_R$ *case*

For the S/F/S case we proceed as in the previous appendix, except that now we have two complications: (i) the electrons and holes in the ferromagnet are coupled due to Andreev reflections, and (ii) more than one combination of basic diagrams in the $2n$th-order expansion ($2n$ scattering events at the S/F interfaces) can give equivalent terms, i.e. the same product of Andreev and normal reflection amplitudes. To demonstrate complication (ii) consider a general closed loop, consisting of the basic processes $x_1, \ldots, x_6$, which contributes to the $2n$th-order expansion

$$x_1^{m_1}x_2^{m_2}x_3^{m_3}x_4^{m_4}x_5^{m_5}x_6^{m_6}, \tag{A.27}$$

with $m_1+m_2+m_3+m_4+2m_5+2m_6 = n$, since x_5 and x_6 have double scattering events at the S/F interfaces. This can be expressed in terms of scattering amplitudes as

$$\tilde{b}_{eR}^{m_1+m_5}\tilde{a}_{eR}^{m_3+m_6}\tilde{b}_{eL}^{m_1+m_6}\tilde{a}_{eL}^{m_4+m_5}\tilde{b}_{hR}^{m_2+m_5}\tilde{a}_{hR}^{m_4+m_6}\tilde{b}_{hL}^{m_2+m_6}\tilde{a}_{hL}^{m_3+m_5}. \tag{A.28}$$

Since x_5x_6 and $x_1x_2x_3x_4$ are expressed by the same product of amplitudes, we can rewrite (A.27) by transferring powers from x_5x_6 to $x_1x_2x_3x_4$ or vice versa. Thus there are several products of basic diagrams which give the same as in (A.28), like

$$x_1^{m_1+k}x_2^{m_2+k}x_3^{m_3+k}x_4^{m_4+k}x_5^{m_5-k}x_6^{m_6-k}, \tag{A.29}$$

where $-m_k \leqslant k \leqslant m_0$ with $m_k = \min(m_1, m_2, m_3, m_4)$ and $m_0 = \min(m_5, m_6)$.

The total number of the closed loops, of the form in (A.29), that gives the same contribution as in (A.28) can be calculated by looking at the scattering events on each vertex (at S/F interfaces). They are normal reflection of electrons (holes) and Andreev reflections from the electron (hole) branch in the F region to the hole (electron) branch in the F region. The possible paths are given by multiplying the combinations of normal reflections out of the total (normal plus Andreev) for both interfaces (L or R) and types of particles (electrons or holes). This gives the product of binomials

$$\begin{aligned}&\binom{(m_1+m_5)+(m_3+m_6)}{m_1+m_5}_{eR}\binom{(m_1+m_6)+(m_4+m_5)}{m_1+m_6}_{eL}\\&\quad\times\binom{(m_2+m_5)+(m_4+m_6)}{m_2+m_5}_{hR}\binom{(m_2+m_6)+(m_3+m_5)}{m_2+m_6}_{hL}.\end{aligned} \tag{A.30}$$

Equivalently, we can start from the power series of Γ with respect to γ, then summing the appropriate factors by the multinomial expansion of the powers of γ with respect to the set of functions $x_1, x_2, x_3, x_4, x_1x_2, x_3x_4, x_5, x_6$ which corresponds to the product in (A.27) and (A.28). From the multinomial expansion of powers of γ we obtain terms like $x_1^{(m_1-i)}x_2^{(m_2-i)}(x_1x_2)^i$, which are included in the coefficient of all paths that contain $x_1^{m_1}x_2^{m_2}$, and similarly for terms with $x_3^{(m_3-j)}x_4^{(m_4-j)}(x_3x_4)^j$.

The result after some tedious but simple algebra is

$$\sum_{k=-m_k}^{m_0}\sum_{j=0}^{m_j+k}\sum_{i=0}^{m_i+k}\frac{(-1)^{m_i+m_j-i-j}(\bar{m}_i+i+\bar{m}_j+j+m_5+m_6)!}{i!(\bar{m}_i-m_i+i)!(m_i-i+k)!\,j!(\bar{m}_j-m_j+j)!(m_j-j+k)!(m_5-k)!(m_6-k)!} \tag{A.31}$$

where $m_i = \min(m_1, m_2)$, $\bar{m}_i = \max(m_1, m_2)$, $m_j = \min(m_3, m_4)$, $\bar{m}_j = \max(m_3, m_4)$ and $m_0 = \min(m_5, m_6)$. We have verified arithmetically that this sum is equal to the products of the binomials in (A.30). Thus the closed path diagrams can be summed by rearrangement to complete powers of γ, so that Γ has the form in (22), with γ given in (21).

A.5. SFFFS case

When we consider a junction with three intermediate ferromagnetic layers a new possibility of closed loops arises, that is loops where all SF vertices are inactive. These loops are included in the term γ_0 in (32), which must be added to the denominator Γ in (31).

Next we examine the case where one SF vertex is active. If the electron vertex at the left interface is active, then the second intermediate vertex at the interface (F_2/F_3) must be disconnected from the right S/F interface, while all intermediate vertices on the hole path are inactive. The first intermediate vertex (F_1/F_2) can either be disconnected from the F_2/F_3 interface or be connected to it, where the three loops shown can be summed to

$$\tilde{b}_{eL}\left(\tilde{r}^e_{12} - g^e_{N12}\tilde{r}^e_{23}\right) \equiv \tilde{b}_{eL}f^e_{N12},$$

where we defined the quantity $f^e_{N12} = \tilde{r}^e_{12} - g^e_{N12}\tilde{r}^e_{23}$. Considering all loops with one active SF interface we have

$$\gamma_1 = \sum_p \tilde{b}_{pL}\big(\tilde{r}^p_{12} - g^p_{N12}\tilde{r}^p_{23}\big)\big(1 - \big(\tilde{r}^{\bar{p}}_{12}\big)'\tilde{r}^{\bar{p}}_{23}\big) + \sum_p \tilde{b}_{pR}\big(\big(\tilde{r}^p_{23}\big)' - g^p_{N23}\big(\tilde{r}^p_{12}\big)'\big)\big(1 - \big(\tilde{r}^{\bar{p}}_{12}\big)'\tilde{r}^{\bar{p}}_{23}\big)$$
$$= \sum_p \tilde{b}_{pL} f^p_{N12}\Gamma^{\bar{p}}_{N1} + \sum_p \tilde{b}_{pR}\big(f^p_{N23}\big)'\Gamma^{\bar{p}}_{N1}, \tag{A.32}$$

where the summation over p includes also the similar loop for the hole and the second summation comes from the right S/F interface and $\bar{p}$ is defined previously. We use the short hand notation

$$f^p_{N12} = \tilde{r}^p_{12} - g^p_{N12}\tilde{r}^p_{23} \tag{A.33}$$
$$\big(f^p_{N23}\big)' = \big(\tilde{r}^p_{23}\big)' - g^p_{N23}\big(\tilde{r}^p_{12}\big)', \tag{A.34}$$

which vanish for the two layers and can be considered as including the closed paths that connect the interface with the closest S/F interface. The quantity

$$\Gamma^p_{N1} = 1 - \big(\tilde{r}^p_{12}\big)'\tilde{r}^p_{23}, \tag{A.35}$$

is the denominator for a three layer junction with normal leads ($N_L/N_1/N_R$).

In (A.32) we considered only one loop in each layer for a given particle. The higher order loops arise from the development of the denominator in powers of γ and therefore are included. The correctness of this approach has been checked in two ways. First by computer algebraic summation of the different closed paths and second by the evaluation of the total scattering matrix. This is rule (e) stated earlier and we keep it all along. This rule enters only when we deal with three or more ferromagnetic layers. Thus in the first (or second) term in (A.32) we include the factor $\Gamma^{\bar{p}}_{N1} = \big(1 - \big(\tilde{r}^{\bar{p}}_{12}\big)'\tilde{r}^{\bar{p}}_{23}\big)$, which adds closed loops in the hole path (for $p = e$) but not the factor $\Gamma^p_{N1} = \big(1 - \big(\tilde{r}^p_{12}\big)'\tilde{r}^p_{23}\big)$ which adds loops in the electron path.

When two SF vertices are active we have again the same possibilities as in the previous case. They are either both vertices at the same interface active or one vertex at each interface. Again when they are on different interfaces they can be either on the same side (electron or hole paths) or at different sides. Of course we also have the two loops which involve one Andreev reflection at each interface. Let us examine the different groups of closed loops of γ_2. Suppose that both SF vertices at the left interface are active, then the second intermediate vertices (F_2/F_3) at the electron and hole paths must be single linked and the first intermediate vertices (at F_1/F_2) can either be doubly or single linked, so they can be described by f^e_{N12} or f^h_{N12} for the electron or hole path correspondingly. The contribution of these kind of loops, taking into account the signs, are

$$-g_L f^e_{N12} f^h_{N12} - g_R f^e_{N23} f^h_{N23}.$$

Now when both SF vertices are active at the same side at each interface the two intermediate vertices can either both be doubly linked or both be single-linked. The quantity that describes the two active SF vertices on the same side is for this case

$$h^p_N = \tilde{r}^p_{12}\big(\tilde{r}^p_{23}\big)' - g^p_{N12}g^p_{N23}. \tag{A.36}$$

Thus the contribution of these kind of loops in the denominator is

$$\sum_p \tilde{b}_{pL}\tilde{b}_{pR}h^p_N.$$

When the two active SF vertices are on different sides the contribution is

$$\sum_p \tilde{b}_{pL} f^p_{N12} \tilde{b}_{\bar{p}R} f^{\bar{p}}_{N23}. \tag{A.37}$$

Considering also the two loops with Andreev scattering at the interfaces γ_2 is

$$\gamma_2 = -g_L f^e_{N12} f^h_{N12} - g_R f^e_{N23} f^h_{N23} - \sum_p \tilde{b}_{pL}\tilde{b}_{pR} h^p_N \Gamma^{\bar{p}}_{N1} - \sum_p \tilde{b}_{pL} f^p_{N12} \tilde{b}_{\bar{p}R} f^{\bar{p}}_{N23} + \tilde{a}_{hL}\left(\tilde{t}^h_{12}\right)'\left(\tilde{t}^h_{23}\right)'\tilde{a}_{eR}\tilde{t}^e_{23}\tilde{t}^e_{12} + \tilde{a}_{eL}\left(\tilde{t}^e_{12}\right)'\left(\tilde{t}^e_{23}\right)'\tilde{a}_{hR}\tilde{t}^h_{23}\tilde{t}^h_{12}. \tag{A.38}$$

When three SF interfaces are active for the path, where both SF vertices are active the intermediate vertices can either both be double or both single linked, and for the remaining SF vertex one intermediate vertex is single linked and the other is either double or single linked. Thus the contribution to the denominator is

$$\gamma_3 = \sum_p \left(\tilde{g}_L \tilde{b}_{pR} h^p_N f^{\bar{p}}_{N12}\right) + \sum_p \left(\tilde{g}_R \tilde{b}_{pL} h^p_N f^{\bar{p}}_{N23}\right). \tag{A.39}$$

Finally, the contribution in the denominator when all SF vertices are active is

$$\gamma_4 = -g_L g_R h^e_N h^h_N. \tag{A.40}$$

The summation of the diagrams seems at first to risk errors. While it is true that care is required, we would like to persuade the reader that it is systematic. To this effect we will eliminate the F_1/F_2 and F_2/F_3 interface scattering amplitudes in favor of the compound scattering amplitudes for $F_1/F_2/F_3$. To this effect we note the following relations:

$$\tilde{r}^p_{13} = \frac{f^p_{N12}}{\Gamma^p_{N1}}, \qquad \left(\tilde{r}^p_{13}\right)' = \frac{f^p_{N23}}{\Gamma^p_{N1}}, \qquad g^p_{N13} = \frac{h^p_N}{\Gamma^p_{N1}},$$

with the analog definition

$$g^p_{N13} = \tilde{r}^p_{13}\left(\tilde{r}^p_{13}\right)' - \tilde{t}^p_{13}\left(\tilde{t}^p_{13}\right)'. \tag{A.41}$$

These relations easily follow from the consideration of a structure with three normal layers, but can also be verified directly from their definitions and the iterative relations presented in the appendix. From the first approach it is clear that the quantity Γ^p_{N1} in the denominator gives the multiple scatterings for a p particle in the center ferromagnetic layer. The first two expressions are easily seen from the definitions of f^p_{N12}, f^p_{N23} and Γ^p_{N1} in (A.33), (A.34) and (A.35) correspondingly. For the third relation again we start from the definitions of h^p_N and g^p_{N13} in (A.36) and (A.41) separately and compare them.

Thus using the above relations we can rewrite the γ_i contributions as

$$\gamma_1 = (1-\gamma_0)\sum_p \tilde{b}_{pL}\tilde{r}^p_{13} + (1-\gamma_0)\sum_p \tilde{b}_{pR}\left(\tilde{r}^p_{13}\right)'. \tag{A.42}$$

where we divided by

$$\Gamma^e_{N1}\Gamma^h_{N1} = (1-\gamma_0)$$

and

$$\frac{\gamma_2}{(1-\gamma_0)} = -g_L\tilde{r}^e_{13}\tilde{r}^h_{13} - g_R\left(\tilde{r}^e_{13}\right)'\left(\tilde{r}^h_{13}\right)' - \sum_p \tilde{b}_{pL}\tilde{b}_{pR} g^p_{N13} - \sum_p \tilde{b}_{pL}\tilde{b}_{\bar{p}R}\tilde{r}^p_{13}\left(\tilde{r}^{\bar{p}}_{13}\right)' + \tilde{a}_{hL}\left(\tilde{t}^h_{13}\right)'\tilde{a}_{eR}\tilde{t}^e_{13} + \tilde{a}_{eL}\left(\tilde{t}^e_{13}\right)'\tilde{a}_{hR}\tilde{t}^h_{13}, \tag{A.43}$$

where we factored out $(1-\gamma_0)$ and in the last two terms we used the relations

$$\tilde{t}^p_{12}\tilde{t}^p_{23} = \left(\tilde{t}^p_{13}\right)\Gamma^p_{N1}, \qquad \left(\tilde{t}^p_{12}\right)'\left(\tilde{t}^p_{23}\right)' = \left(\tilde{t}^p_{13}\right)'\Gamma^p_{N1},$$

from the iteration relations for the scattering amplitudes in the intermediate layers.

$$\frac{\gamma_3}{(1-\gamma_0)} = \sum_p g_L g^p_{N13} \tilde{b}_{pR} \tilde{r}^{\bar{p}}_{13} + \sum_p g_R g^p_{N13} \tilde{b}_{pL} \left(\tilde{r}^{\bar{p}}_{13}\right)' \tag{A.44}$$

$$\frac{\gamma_4}{(1-\gamma_0)} = -g_L g_R g^e_{N13} g^h_{N13}. \tag{A.45}$$

Thus the denominator for the S/F/F/F/S case (Γ_{S3}) is simply related to the one for S/F/F/S (Γ_{S2}, with the amplitudes r_{13} etc.) by the following $\Gamma_{S3} = (1-\gamma_0)\Gamma_{S2}$.

A.6. Scattering matrix method

A.6.1. Scattering amplitudes of the $S_1/F_1/F_n/S_2$ *junction.* The scattering matrix of the multiferromagnetic junction can be obtained as a function of the scattering amplitudes of FS barriers ($a, b, c, d, a^*, b^*, c^*, d^*$) and F_iF_{i+1}-barriers ($r_{i,i+1}, t_{i,i+1}, r'_{i,i+1}, t'_{i,i+1}$).

The problem one has to solve is the $S_1/F_1/F_n/S_2$ junction. First we express the reflection and transmission coefficients ($A, B, C, D, A', B', C', D'$) of the whole junction in terms of the scattering amplitudes ($a, b, c, d, a^*, b^*, c^*, d^*$) at the S/F interfaces and the $F_1/\cdots/F_n$ interface scattering amplitudes ($r_{1n}, t_{1n}, r'_{1n}, t'_{1n}$). Then we use the composition procedure for the n-non-superconducting regions, as described in the following section, and substitute the results for $r_{1n}, t_{1n}, r'_{1n}, t'_{1n}$ by the amplitudes $r_{1,i}, t_{1,i}, r'_{1,i}, t'_{1,i}$ for $i = 1, 2, \ldots (n-1)$ which must be evaluated consecutively. This means that we replace the interior sequence of the F-layers ($F_1/F_2/\ldots/F_n$) which is characterized by the amplitudes $r_{12}, \ldots, r_{n-1n}, t_{12}, \ldots, t_{n-1,n}, r'_{12}, \ldots, r'_{n-1,n}, t'_{12}, \ldots, t'_{n-1,n}$ with the sequence (F_1/F_n) which is characterized by $r_{1n}, t_{1n}, r'_{1n}, t'_{1n}$.

A.6.2. Scattering matrix of the SFFS junction. The matching conditions at the three interfaces of the $S_1/F_1/F_n/S_2$ gives the following set of equations

$$\begin{pmatrix} \chi^r_{n-} \\ \psi^R_+ \end{pmatrix} = \left(\begin{array}{c|c} \hat{R}_2 & \hat{T}_2^{\,*} \\ \hline \hat{T}_2 & \hat{R}_2^{\,*} \end{array}\right) \begin{pmatrix} \chi^r_{n+} \\ \psi^R_- \end{pmatrix} \tag{A.46}$$

$$\begin{pmatrix} \chi^r_{1-} \\ \chi^l_{n+} \end{pmatrix} = \left(\begin{array}{c|c} \hat{r}_{1n} & \hat{t}'_{1n} \\ \hline \hat{t}_{1n} & \hat{r}'_{1n} \end{array}\right) \begin{pmatrix} \chi^r_{1+} \\ \chi^l_{n-} \end{pmatrix} \tag{A.47}$$

$$\begin{pmatrix} \psi^L_- \\ \chi^l_{1+} \end{pmatrix} = \left(\begin{array}{c|c} \hat{R}_1^{\,*} & \hat{T}_1 \\ \hline \hat{T}_1^{\,*} & \hat{R}_1 \end{array}\right) \begin{pmatrix} \psi^L_+ \\ \chi^l_{1-} \end{pmatrix}, \tag{A.48}$$

where $\chi_1(\chi_n)$ is the spinor vector of the region $F_1(F_n)$, $\psi^L(\psi^R)$ the spinor vector of the left(right) superconductor $S_1(S_2)$, the subscript $+(-)$ stands for right(left) moving particles and the superscript $l(r)$ for the left(right) side of the segment 1 or n. Expressing all spinors with respect to the incoming quasiparticles, the equations for the outgoing quasiparticles can be written as

$$\begin{pmatrix} \psi^L_- \\ \psi^R_+ \end{pmatrix} = \left(\begin{array}{c|c} \hat{R}_{L\to R} & \hat{T}'_{L\to R} \\ \hline \hat{T}_{L\to R} & \hat{R}'_{L\to R} \end{array}\right) \begin{pmatrix} \psi^L_+ \\ \psi^R_- \end{pmatrix}, \tag{A.49}$$

where $\hat{R}_{L\to R}$, $\hat{T}_{L\to R}$ contains the elements

$$\hat{R}_{L\to R} = \left(\begin{array}{c|c} B_e & A_h \\ \hline A_e & B_h \end{array}\right), \qquad \hat{T}_{L\to R} = \left(\begin{array}{c|c} C_e & D_h \\ \hline D_e & C_h \end{array}\right). \tag{A.50}$$

After some calculations we derive from equations (12)–(14) for the $\hat{T}_{L\to R}$ (for example) the following:

$$\begin{aligned}\hat{T}_{L\to R} = &-\hat{T}_2\tau_n\hat{t}_{1n}\tau_1(1-(\hat{R}_2\tau_n\hat{t}_{1n}\tau_1)^{-1}(1-\hat{R}_2\tau_n\hat{r}'_{1n}\tau_n)(\hat{R}_1\tau_1\hat{t}'_{1n}\tau_n)^{-1}(1-\hat{R}_1\tau_1\hat{r}_{1n}\tau_1))^{-1}\\ &\times(\hat{R}_2\tau_n\hat{t}_{1n}\tau_1)^{-1}(1-\hat{R}_2\tau_n\hat{r}'_{1n}\tau_n)(\hat{R}_1\tau_1\hat{t}'_{1n}\tau_n)^{-1}\hat{T}'_1-\hat{T}_2\tau_n\hat{r}'_{1n}\tau_n\\ &\times(1-(\hat{R}_1\tau_1\hat{t}'_{1n}\tau_n)^{-1}(1-\hat{R}_1\tau_1\hat{r}_{1n}\tau_1)(\hat{R}_2\tau_n\hat{t}_{1n}\tau_1)^{-1}(1-\hat{R}_2\tau_n\hat{r}'_{1n}\tau_n))^{-1}\\ &\times(\hat{R}_1\tau_1\hat{t}'_{1n}\tau_n)^{-1}\hat{T}'_1,\end{aligned}$$

where

$$\tau_1=\begin{pmatrix}\mathrm{e}^{\mathrm{i}q_{e1}d_1} & \\ & \mathrm{e}^{-\mathrm{i}q_{h1}d_1}\end{pmatrix},\qquad \tau_n=\begin{pmatrix}\mathrm{e}^{\mathrm{i}q_{en}d_n} & \\ & \mathrm{e}^{-\mathrm{i}q_{hn}d_n}\end{pmatrix} \tag{A.51}$$

are the propagation matrices of regions F_1 and F_n correspondingly. That means for the right- and left-going particles

$$\chi^r_{1(n)+}=\tau_{1(n)}\chi^l_{1(n)+},\qquad \chi^l_{1(n)-}=\tau_{1(n)}\chi^r_{1(n)-}.$$

Defining the tilde matrices as the product of an scattering event matrix and a propagation matrix of a region before the event happens

$$\tilde{S}=\hat{S}\tau, \tag{A.52}$$

where S stands for r, t, R, T etc and using the identity

$$(1-AB)^{-1}=-B^{-1}(1-A^{-1}B^{-1})^{-1}, \tag{A.53}$$

we derive after some simple algebra the formula

$$\hat{T}_{L\to R}=\tilde{T}_2(1-\tilde{r}'_{1n}\tilde{R}_2)^{-1}\tilde{t}_{1n}(1-(\tilde{R}_1\tilde{t}'_{1n})(1-\tilde{R}_2\tilde{r}'_{1n})^{-1}(\tilde{R}_2\tilde{t}_{1n})(1-\tilde{R}_1\tilde{r}_{1n})^{-1})^{-1}\hat{T}^*_1. \tag{A.54}$$

In a similar manner we derive

$$\hat{T}'_{L\to R}=\tilde{T}_1(1-\tilde{r}_{1n}\tilde{R}_1)^{-1}\tilde{t}'_{1n}(1-(\tilde{R}_2\tilde{t}_{1n})(1-\tilde{R}_1\tilde{r}_{1n})^{-1}(\tilde{R}_1\tilde{t}'_{1n})(1-\tilde{R}_2\tilde{r}'_{1n})^{-1})^{-1}\hat{T}^*_2 \tag{A.55}$$

$$\begin{aligned}\hat{R}_{L\to R}=&\hat{R}^*_1+\tilde{T}_1(\tilde{r}_{1n}+\tilde{t}'_{1n}\tilde{R}_2(1-\tilde{r}'_{1n}\tilde{R}_2)^{-1}\tilde{t}_{1n})(1-\tilde{R}_1\tilde{r}_{1n})^{-1}\\ &\times(1-(\tilde{R}_1\tilde{t}'_{1n})(1-\tilde{R}_2\tilde{r}'_{1n})^{-1}(\tilde{R}_2\tilde{t}_{1n})(1-\tilde{R}_1\tilde{r}_{1n})^{-1})^{-1}\hat{T}^*_1\end{aligned} \tag{A.56}$$

$$\begin{aligned}\hat{R}'_{L\to R}=&\hat{R}^*_2+\tilde{T}_2(\tilde{r}'_{1n}+\tilde{t}_{1n}\tilde{R}_1(1-\tilde{r}_{1n}\tilde{R}_1)^{-1}\tilde{t}'_{1n})(1-\tilde{R}_2\tilde{r}'_{1n})^{-1}\\ &\times(1-(\tilde{R}_2\tilde{t}_{1n})(1-\tilde{R}_1\tilde{r}_{1n})^{-1}(\tilde{R}_1\tilde{t}'_{1n})(1-\tilde{R}_2\tilde{r}'_{1n})^{-1})^{-1}\hat{T}^*_2.\end{aligned} \tag{A.57}$$

In the evaluation of the inverse matrices in (A.56) and (A.57) we obtain two determinants, which turn out to be equal, i.e.

$$\begin{aligned}\frac{\Gamma}{\Gamma_D}&=det(1-(\tilde{R}_1\tilde{t}'_{1n})(1-\tilde{R}_2\tilde{r}'_{1n})^{-1}(\tilde{R}_2\tilde{t}_{1n})(1-\tilde{R}_1\tilde{r}_{1n})^{-1})\\ &=det(1-(\tilde{R}_2\tilde{t}_{1n})(1-\tilde{R}_1\tilde{r}_{1n})^{-1}(\tilde{R}_1\tilde{t}'_{1n})(1-\tilde{R}_2\tilde{r}'_{1n})^{-1}),\end{aligned}$$

where $\Gamma_D=g_Lg_R\tilde{t}^e_{1n}\tilde{t}^h_{1n}\left(\tilde{t}^e_{1n}\right)'\left(\tilde{t}^h_{1n}\right)'$.

This determinant is the one that includes all the important closed paths, as discussed in the text, and is proportional to the denominator Γ, whose vanishing give us the Andreev spectrum.

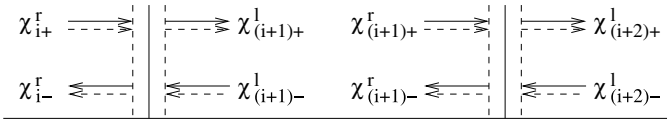

Figure 20. Basic processes corresponding to (A.58) and (A.59).

A.6.3. Composition of the scattering matrix of the ferromagnet multilayer. At an F_i/F_{i+1} interface (of barrier strength Z_i) between two neighboring normal regions i and $i+1$ the amplitudes χ_i and χ_{i+1} are related by the following equations:

$$\begin{pmatrix} \chi^r_{i-} \\ \chi^l_{(i+1)+} \end{pmatrix} = \left(\begin{array}{c|c} \hat{r}_{i,i+1} & \hat{t}'_{i,i+1} \\ \hline \hat{t}_{i,i+1} & \hat{r}'_{i,i+1} \end{array}\right) \begin{pmatrix} \chi^r_{i+} \\ \chi^l_{(i+1)-} \end{pmatrix}, \tag{A.58}$$

where the superscripts r or l denote the amplitude at the left end or the right end of each layer. The two are related by the corresponding diagonal propagation matrices as shown in figure 20, with the electron or hole propagation phase.

If we consider the next region $i+2$, we write

$$\begin{pmatrix} \chi^r_{(i+1)-} \\ \chi^l_{(i+2)+} \end{pmatrix} = \left(\begin{array}{c|c} \hat{r}_{i+1,i+2} & \hat{t}'_{i+1,i+2} \\ \hline \hat{t}_{i+1,i+2} & \hat{r}'_{i+1,i+2} \end{array}\right) \begin{pmatrix} \chi^r_{(i+1)+} \\ \chi^l_{(i+2)-} \end{pmatrix}. \tag{A.59}$$

Combining these sets of equations we can relate the statevector χ_i of region i with the statevector χ_{i+2} of region $i+2$:

$$\begin{pmatrix} \chi^r_{i-} \\ \chi^l_{(i+2)+} \end{pmatrix} = \left(\begin{array}{c|c} \hat{r}_{i,i+2} & \hat{t}'_{i,i+2} \\ \hline \hat{t}_{i,i+2} & \hat{r}'_{i,i+2} \end{array}\right) \begin{pmatrix} \chi^r_{i+} \\ \chi^l_{(i+2)-} \end{pmatrix} \tag{A.60}$$

where

$$\begin{aligned}
\hat{t}_{i,i+2} &= (\hat{t}_{i+1,i+2}\tau_{i+1})(1-(\hat{r}'_{i,i+1}\tau_{i+1})(\hat{r}_{i+1,i+2}\tau_{i+1}))^{-1}\hat{t}_{i,i+1} \\
\hat{r}'_{i,i+2} &= \hat{r}'_{i+1,i+2} + (\hat{t}_{i+1,i+2}\tau_{i+1})(1-(\hat{r}'_{i,i+1}\tau_{i+1})(\hat{r}_{i+1,i+2}\tau_{i+1}))^{-1}(\hat{r}'_{i,i+1}\tau_{i+1})\hat{t}'_{i+1,i+2} \\
\hat{r}_{i,i+2} &= \hat{r}_{i,i+1} + (\hat{t}'_{i,i+1}\tau_{i+1})(\hat{r}_{i+1,i+2}\tau_{i+1})(1-(\hat{r}'_{i,i+1}\tau_{i+1})(\hat{r}_{i+1,i+2}\tau_{i+1}))^{-1}\hat{t}_{i,i+1} \\
\hat{t}'_{i,i+2} &= (\hat{t}'_{i,i+1}\tau_{i+1})(1-(\hat{r}_{i+1,i+2}\tau_{i+1})(\hat{r}'_{i,i+1}\tau_{i+1}))^{-1}\hat{t}'_{i+1,i+2}.
\end{aligned}$$

Thus we have an iterative scheme to obtain consecutively from the (12) $\rightarrow$ (13) $\rightarrow \cdots \rightarrow (1n)$ scattering matrices for the total scattering matrix from the ferromagnetic layers. It should be remarked that one can treat a very general ferromagnetic layer whose physical parameters can be approximated piecewise constant.

References

[1] Andreev A F 1964 *Sov. Phys.—JETP* **19** 1228
[2] Blonder G E, Tinkham M and Klapwijk T M 1983 *Phys. Rev.* B **25** 4515
[3] Beenaker C W J 1991 *Phys. Rev. Lett.* **67** 3836
[4] Bagwell P F 1992 *Phys. Rev.* B **46** 12573
[5] Chrestin A, Matsuyama T and Merkt U 1994 *Phys. Rev.* B **49** 498
[6] Shumeiko V S and Bratus E N 1997 *Low Temp. Phys.* **23** 181
[7] Bulaevskii L N, Kuzii V V and Sobyanin A A 1977 *JETP Lett.* **25** 290
[8] de Jong M J M and Beenaker C W J 1995 *Phys. Rev. Lett.* **74** 1657
[9] Buzdin A 2000 *Phys. Rev.* B **62** 11377
[10] Buzdin A I 2005 *Rev. Mod. Phys.* **77** 935
[11] Golubov A G, Kupriyanov M Yu and Llichev E 2004 *Rev. Mod. Phys.* **76** 411

[12] Cayssol J and Montambaux G 2004 *Phys. Rev.* **70** 224520
[13] Chtchelkatchev N M, Belzig W, Nazarov Yu V and Bruder C 2001 *JETP Lett.* **74** 323
[14] Furusaki A and Tsukada M 1991 *Solid State Commun.* **78** 299
[15] Bozovic I 2001 *IEEE Trans. Appl. Supercond.* **11** 2886
[16] Ryazanov V V, Oboznov V A, Rusanov A Yu, Veretennikov A V, Golubov A A and Aarts J 2001 *Phys. Rev. Lett.* **86** 2427
[17] Kontos T, Aprili M, Lesueur J and Grison X 2001 *Phys. Rev. Lett.* **86** 304. SIFS
[18] Blum Y, Tsukernik A, Karpoviski M and Palevski A 2002 *Phys. Rev. Lett.* **89** 187004
[19] Sellier H, Baraduc C, Lefloch F and Calemczuk R 2004 *Phys. Rev. Lett.* **92** 257005
[20] Bergeret F S, Volkov A F and Evetov K B 2001 *Phys. Rev.* B **64** 134506
[21] Chtchelkatchev N M, Belzig W, Nazarov Yu V and Bruder C 2001 *JETP Lett.* **74** 323
[22] Radovic Z, Lazarides N and Flytzanis N 2003 *Phys. Rev.* B **68** 014501
[23] Tang H X, Wang Z D and Zhang Y 1996 *Zeit. Phys.* B **101** 359
[24] Chtchelkatchev N M 2004 *JETP Lett.* **80** 743
[25] Mohammadkhani G and Zareyan M 2006 *Phys. Rev.* B **73** 134503
[26] Baselmans J J A, Morpurgo A F, Wees B J van and Klapwijk T M 1999 *Nature (London)* **397** 43
[27] Tsuei C C and Kirtley J R 2000 *Rev. Mod. Phys.* **72** 969
[28] Wollman D A, Harlingen D J Van, Giapintzakis J and Ginsberg D M 1995 *Phys. Rev. Lett.* **74** 797
[29] Smilde H J H, Blank D H A, Gerritsma G J, Hilgenkamp H and Rogalla H 2002 *Phys. Rev. Lett.* **88** 057004
[30] Hildgenkamp H, Ariando, Smilde H J H, Blank D H A, Rijnders G, Rogalla H, Kirtley J R and Tsuei C C 2003 *Nature (London)* **422** 50
[31] Yamashita T, Takahashi S and Maekawa S 2006 *Phys. Rev.* B **73** 144517
[32] Koshina E A and Krivoruchko V N 2001 *Phys. Rev.* B **63** 224515
[33] Krivoruchko V N and Koshina E A 2001 *Phys. Rev.* B **64** 172511
[34] Golubov A A, Kupriyanov M Yu and Fominov Ya V 2002 *JETP Lett.* **75** 223
[35] Blanter Ya M and Hekking F W J 2004 *Phys. Rev.* B **69** 024525
[36] Paltoglou V, Margaris I and Flytzanis N 2006 *J. Phys. A: Math. Gen.* **39** 1
[37] Paltoglou V, Margaris I and Flytzanis N 2007 *Mod. Phys. Lett.* B **21** 505
[38] Petkovic I, Chtchelkatchev N M and Radovic Z 2006 *Phys. Rev.* B **73** 184510
[39] Nevirkovets I P and Ketterson J B 2000 *JETP Lett.* **71** 342